# Anisotropic size effects in semiconductors and semimetals

É. I. Rashba

*L. D. Landau Institute of Theoretical Physics, USSR Academy of Sciences, Chernogolovka (Moscow Province)*

Z. S. Gribnikov

*Institute of Semiconductors, Ukrainian Academy of Sciences, Kiev*

V. Ya. Kravchenko

*Institute of Solid State Physics, USSR Academy of Sciences, Chernogolovka (Moscow Province)*
Usp. Fiz. Nauk **119**, 3–47 (May 1976)

Large differences between the characteristic times of various electronic relaxation processes (momentum relaxation, energy relaxation, intervalley relaxation, electron-hole recombination) make it possible to divide carriers into groups between which relaxation is relatively slow. Each of the "long" relaxation times can be matched by a characteristic diffusion length which is much greater than the usual mean free path. Transport coefficients of such groups are generally anisotropic even in cubic crystals and the anisotropy varies from group to group (this anisotropy may be natural or it may be induced by pressure, magnetic field. etc.). Therefore, the passage of a current produces nonequilibrium carrier densities in such groups. The density gradients are oriented at right-angles to the current and they decay over distances of the order of the diffusion length. The effects associated with the formation of nonequilibrium carriers and the influence of their diffusion on the transport coefficients are referred to in the paper as the anisotropic size effects. The paper reviews experimental and theoretical investigations of various manifestations of such effects. An analysis is made of the size dependences of the electrical conductivity and magnetoresistance manifested in "thick" samples (thickness of the order of the diffusion length). Other topics considered include nonlinearity of the electrical conductivity in relatively weak fields, redistribution of carriers in "strong" fields (accompanied by giant changes in the total number of carriers and by formation of domains, depletion layers, and accumulation layers), influence of the anisotropic size effects on the skin effect (which changes the surface impedance of semimetals by an order of magnitude), and electromagnetic excitation of sound in semimetals.

PACS numbers: 72.20.My, 72.20.Fr, 72.10.−d

## CONTENTS

Introduction . . . 361
1. Mechanisms of Anisotropic Size Effects . . . 362
2. Anisotropic Size Effects in Weak Electric Fields . . . 365
3. Electrical Pinch Effect in Ambipolar Semiconductors . . . 374
4. Many-Valley Crystal in Strong Fields . . . 378
5. Skin Effect in Semimetals . . . 381
Conclusions . . . 383
Literature Cited . . . 384

## INTRODUCTION

Solids always exhibit a hierarchy of electronic relaxation times representing the rates of recovery of equilibrium by an electronic system. A very important point to note is that the differences between the characteristic times of various relaxation process may be very large, particularly in semiconductors. Typical examples are the momentum relaxation time $\tau_p$, energy relaxation time $\tau$, intervalley relaxation time $\tau_v$, and electron-hole recombination time $\tau_r$. The shortest of these is the momentum relaxation time $\tau_p \sim 10^{-9}-10^{-12}$ sec; the times $\tau$ and $\tau_v$ are often two or three orders of magnitude longer and the time $\tau_r$ can be six to nine orders of magnitude greater than the momentum relaxation time. Each of the "long" relaxation times can be matched by a characteristic diffusion length: $L_\varepsilon \sim \sqrt{D\tau_\varepsilon}$, $L_v \sim \sqrt{D\tau_v}$, $L_r \sim \sqrt{D\tau_r}$; here, $D$, is the diffusion coefficient. If $\tau_p$ is the shortest of these times, all these diffusion lengths exceed considerably $l_p \sim \sqrt{D\tau_p} \sim v\tau_p$, which is the usual mean free path ($v$ is the typical electron velocity). These large differences between the relaxation times make it possible to divide carriers into groups between which relaxation is slow; we shall make such a division later.

In the linear theory of the transport phenomena in homogeneous media, the dominant influence is exerted by the shortest of these times and the influence of all the other relaxation mechanisms is usually slight.[1)]

The situation is quite different in the case of size effects: since the largest characteristic lengths are associated with the longest relaxation times, it follows

[1)]One of the exceptions is the low-temperature resistance of pure metals, which is controlled by umklapp processes[149,150]; we shall not consider such cases.

 Copyright © 1977 American Institute of Physics 

that, when a sample is reduced in thickness, these relaxation lengths are the first to become comparable with the geometric dimensions of the sample and, therefore, the size effects begin to be manifested in the phenomena described by these lengths. Only in the case of the thinnest samples do we observe the usual size effect[1] associated with $l_p$.

Since the relaxation length corresponding to the electron–hole recombination in semiconductors reaches ~1 cm, trivial size effects such as the dependence of the photoconductivity on the dimensions of a sample can easily be observed experimentally.[2)] We wish to stress here those features of the generation of nonequilibrium carriers and their spatial distribution which are typical of anisotropic size effects. Nonequilibrium carriers are usually either generated by external sources (illuminated spot) or are injected across a $p$–$n$ junction, so that the density gradient is oriented along the current. In anisotropic size effects discussed below, we shall assume that the current itself generates nonequilibrium carriers on the lateral faces of a sample[3)] and, therefore, the density gradients are normal to the direction of the current. The condition for the appearance of nonequilibrium carriers is the presence of anisotropic groups of carriers for which the current is directed at an angle relative to the applied electric field. The anisotropy can be natural or generated by pressure, magnetic field, etc. Nonequilibrium densities established near the boundaries disappear over distances of the order of the corresponding relaxation lengths $L$ and size effects can be observed over distances $d \lesssim L$, where $d$ is the geometric dimension. Therefore, anisotropic size effects can be used to measure large relaxation lengths (or, which is equivalent, the rates of slow relaxation processes).

Each of the anisotropic size effects not only has a bulk relaxation time which governs—via the corresponding diffusion length—the spatial scale of the effect, but also a definite surface relaxation rate such as the degree of diffuseness of the surface scattering, rate of surface cooling of carriers, and rate of intervalley scattering and recombination. The surface relaxation mechanisms involving short characteristic lengths are practically unimportant in the size effects which are larger on the spatial scale; for example, the diffuseness of the surface scattering should not influence the effects associated with the relaxation lengths $L_\varepsilon$, $L_v$, and $L_r$. The special feature of the anisotropic size effects is that they are maintained and sometimes have maximum values when the corresponding surface relaxation mechanism becomes unimportant and they disappear completely in homogeneous samples if the rate of relaxation on the whole outer surface increases without limit. Conversely, the traditional size effects (see, for example, [11]) appear due to surface relaxation and are no longer observed when the relaxation disappears on the whole surface. We shall show later that nonlinear anisotropic size effects are strongest when the relaxation rates differ considerably from one face of a sample to another.

Related effects also appear in the course of propagation of electromagnetic waves, which should be accompanied by carrier density waves. Here, the role of $d$ is played by the wavelength $\lambda$ (or the skin depth $\delta$).

## 1. MECHANISMS OF ANISOTROPIC SIZE EFFECTS

We shall use the concept of a "carrier group" in the following sense: the relaxation time between groups of carriers should be considerably greater than the relaxation time within a group. We shall discuss in detail the following examples of groups: a) carriers belonging to different valleys in the case of a many-valley energy spectrum (such as that exhibited by electrons in Bi, Ge, Si, and GaP, by electrons and holes in lead chalcogenides, etc.); b) carriers with different kinetic energies within one band (or one valley); c) carriers belonging to different bands (for example, electrons and holes). However, this list can be continued to cover electrons with a specific spin orientation, or electrons belonging to one part of a multiply connected Fermi surface of a metal. Sometimes, the anisotropy of individual groups is created by the application of a magnetic field.

If the relaxation times differ very greatly, then each group may be assigned a separate set of transport coefficients such as the mobility tensor $\hat{u}^\alpha$, tensor of the diffusion coefficients $\hat{D}^\alpha$, conductivity tensor $\hat{\sigma}^\alpha$, etc.; here, $\alpha$ is the label of a group. It is very important to note that the transport coefficients of individual groups are usually strongly anisotropic even in high-symmetry crystals.

In this section, we shall consider several examples to demonstrate the physical factors which can make $\tau_p$ considerably shorter than the other relaxation times and discuss the mechanism as a result of which the presence of anisotropic groups gives rise to nonequilibrium carriers.

### A. Long relaxation times

There is a variety of reasons why $\tau_r$, $\tau_v$, and $\tau_\varepsilon$ may be considerably greater than $\tau_p$; therefore, the absolute and relative values of these "long" relaxation times may vary greatly.

The rate of electron–hole recombination in semiconductors is limited by the need to transfer electron energy of the order of the forbidden band width (~1 eV). The recombination times are in the range $\tau_r \sim 10^{-9}$–$10^{-3}$ sec, depending on the mechanism.[4)]

The electron spectra of semimetals and quite a few semiconductors are of the many-valley type: energy extrema are found at several points in the Brillouin zone. The scattering of an electron from one valley to another involves the transfer of momentum of the order of the Brillouin value and, therefore, the geometric

---

[2)]For details, see, for example, §19 in[151] and[152,153].

[3)]Or on other "transverse" inhomogeneities.

[4)]The discussion of the recombination mechanisms in semiconductors can be found in relevant books.[152–154]

cross section for impurity intervalley scattering is $\sigma \sim 10^{-15}-10^{-16}$ cm$^2$. Allowance for the processes which include capture or exchange scattering results in some increase of these cross sections. For example, in the case of scattering by donors in Ge at $T=4$ °K, we have $\sigma \sim 10^{-13}-10^{-12}$ cm$^2$,[2–4] which are still much smaller than the cross sections for the usual Coulomb scattering under the same conditions ($\sigma \sim 10^{-11}$ cm$^2$). Since the Debye screening radius $l_D$ of semimetals ($l_D \sim 10-100$ Å) is considerably greater than the lattice constant, once again the difference between the probabilities of intravalley and intervalley scattering should be large. Naturally, intervalley phonon scattering processes are also possible. However, they involve the transfer of energy which corresponds to the Debye frequency and, therefore, their probability is exponentially small at low temperatures. It must be stressed that, in the case of semimetals, there is no basic difference between the intervalley electron scattering and electron–hole recombination: the latter process is also limited by the need to transfer a large momentum and the relaxation time is of the same order of magnitude ($\tau_v \sim \tau_r$). According to[5], the relaxation times $\tau_p$ and $\tau_r$ of Bi become equal at $T \approx 15$ °K but at lower temperatures the difference between them reaches two orders of magnitude.

The difference between $\tau_p$ and $\tau_\varepsilon$ is due to the fact that the scattering of electrons by impurities is elastic and that by acoustic phonons is quasielastic. In the latter case, the expansion parameter is $(c_s/v)^2 \ll 1$ ($c_s$ is the velocity of sound). When these mechanisms dominate the momentum dissipation, it is usually found that $\tau_p/\tau_\varepsilon \sim 10^{-3}$.

## B. Physical mechanism of anisotropic size effects

We shall now consider the physical mechanism and the principal features of anisotropic size effects. The experimental geometry is shown in Fig. 1: a sample is assumed to be bounded along the directions $y$ and $z$ but not along $x$; the current flows along the $x$ axis and its average density is $i$. We shall assume that all the times $\tau_{\alpha\beta}$ representing relaxation between groups $\alpha$ and $\beta$ satisfy the criterion $\tau_{\alpha\beta} \gg \tau_p$ and, therefore, different transport tensors $\hat{u}^\alpha$, $\hat{\sigma}^\alpha = en_\alpha \hat{u}^\alpha$, and $\hat{D}^\alpha$ can be attributed to the two groups ($n_\alpha$ is the density of carriers in group $\alpha$, i.e., the density of $\alpha$ electrons). The various vectors can be represented conveniently in the form $\mathbf{A} = \mathbf{A}_x + \mathbf{A}_\perp$, and a similar notation can be introduced for the components of the transport tensors.

We shall consider the currents which are produced by an external electric field $\mathbf{E} = \mathbf{E}_x$ and we shall assume an initially homogeneous distribution in the transverse direction (all $n_\alpha$ = const). Under these conditions, the current is entirely due to the field and, since the tensors $\hat{\sigma}^\alpha$ are anisotropic, the partial currents associated with individual groups $\mathbf{i}^\alpha = \hat{\sigma}^\alpha \mathbf{E}_x$, have nonvanishing transverse components $\mathbf{i}_\perp^\alpha = \hat{\sigma}_{\perp x}^\alpha E_x$.

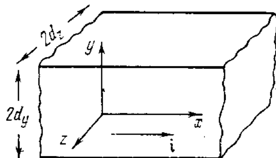


FIG. 1. Experimental geometry.

The situation is simplest in the case when there is only one group of carriers: the resultant transverse current generates a transverse field $\mathbf{E}_\perp$ (quasi-Hall field) such that the current due to the total field $\mathbf{E}$ is entirely longitudinal $\mathbf{i}_\perp^\alpha = (\hat{\sigma}^\alpha \mathbf{E})_\perp = 0$. The carrier density $n_\alpha$ is then constant because of the neutrality condition.

The situation is completely different when the number of carrier groups is more than one. In this case, we can select the vector $\mathbf{E}_\perp$ in such a way that only the total transverse current density vanishes:

$$\mathbf{i}_\perp = (\hat{\sigma}\mathbf{E})_\perp = 0, \quad \hat{\sigma} = \sum_\alpha \hat{\sigma}^\alpha, \tag{1.1}$$

i.e., we can ensure conservation of the electric charge. Then, $\mathbf{E}_\perp$ and the total current are given by[5)]

$$\left.\begin{aligned} \mathbf{E}_\perp &= -(\sigma_{\perp\perp})^{-1}\sigma_{\perp x}E_x, \quad i_x = \Sigma(\infty)E_x, \\ \Sigma(\infty) &= \sigma^* = \sigma_{xx} - \sigma_{x\perp}(\hat{\sigma}_{\perp\perp})^{-1}\sigma_{\perp x}. \end{aligned}\right\} \tag{1.2}$$

The partial transverse currents associated with individual groups are

$$\mathbf{i}_\perp^\alpha = [\sigma_{\perp x}^\alpha - \hat{\sigma}_{\perp\perp}^\alpha(\hat{\sigma}_{\perp\perp})^{-1}\hat{\sigma}_{\perp x}]E_x. \tag{1.3}$$

Deriving, by analogy with Eq. (1.3), the expression (1.1) for the total transverse current $\mathbf{i}_\perp$, we readily see that the partial currents $\mathbf{i}_\perp^\alpha$ vanish together with $\mathbf{i}_\perp$ only if

$$(\hat{\sigma}_{\perp\perp}^\alpha)^{-1}\sigma_{\perp x}^\alpha = \mathrm{C}, \tag{1.4}$$

where C is independent of $\alpha$. The relationship (1.4) is satisfied only exceptionally, for example, when the tensors $\hat{\sigma}^\alpha$ for all the valleys are proportional to one another (all groups have the same anisotropy) or when $\sigma_{\perp x}^\alpha = 0$ for all the groups.

The pattern of the transverse currents of Eq. (1.3) may be stationary only if mechanisms converting carriers of one group ("arriving" carriers) into carriers of other groups ("departing" carriers) act on all surfaces with a practically full efficiency. Such conversion includes intervalley scattering, electron–hole recombination, inelastic scattering of electrons, etc. However, if the rate of such intergroup surface conversion is limited, the initial electron balance is disturbed: each of the surface layers exhibits the accumulation of carriers from some groups and depletion of carriers of other groups. The resultant transverse density gradients give rise to diffusion currents and a new steady state is established only when the partial transverse currents on the surface balance the rate of the intergroup surface scattering. Then, the partial currents should be described by the general formulas

$$\mathbf{i}^\alpha = -e_\alpha \hat{D}^\alpha \nabla n_\alpha + en_\alpha \hat{u}^\alpha \mathbf{E}; \tag{1.5}$$

Here, $e_\alpha = \pm e$ ($e > 0$) for the hole and electron groups, respectively.

Thus, the arriving current generates a spatially inhomogeneous carrier distribution; there is an apparent separation in the $\mathbf{r}$ space of the carriers belonging to

---

5)For a cubic crystal, $\hat{\sigma}$ is naturally a scalar and $\sigma^* = \sigma$.

different groups (for example, those belonging to different valleys in the $\mathbf{p}$ space).

Since there is always some intervalley scattering in the bulk, nonequilibrium carrier densities relax in the direction of the interior of a sample. In weak electric fields, such relaxation occurs over distances equal to the intergroup lengths $L \sim \sqrt{D\tau_{\alpha\beta}}$ (see Sec. 2). Consequently, the carrier densities are perturbed in surface layers $\sim L$ thick but, at greater depths from the surface, they return to their equilibrium values. Therefore, for an arbitrary rate of surface conversion, $\Sigma(\infty)$ represents the conductivity of bulk samples ($d_y$, $d_z \gg L$); this is indicated by the argument $\infty$ in parentheses.

We shall usually assume that all the dimensions are considerably greater than the Debye screening length $l_D$ ($d_y$, $d_z$, $L \gg l_D$). Then, the quasineutrality condition is satisfied practically throughout the bulk of the sample:

$$\sum_\alpha e_\alpha n_\alpha = \text{const.} \tag{1.6}$$

In weak fields $E_x$, when the densities $n_\alpha$ are perturbed only slightly compared with the equilibrium values, the behavior of ambipolar systems (i.e., systems with groups of carriers of different charges) does not differ in any way from the behavior of unipolar systems. The position changes greatly in strong fields: in the case of a unipolar system, the condition (1.6) governs the sum of densities, whereas, in the ambipolar case, it governs the difference $n_+ - n_-$. Therefore, in unipolar systems, certain groups of carriers can replace others without a change in the total number of carriers; consequently, the size effects may be largely due to differences between the mobilities of various groups. On the other hand, in ambipolar systems, we may have extensive accumulation and depletion regions, and the resistance may change by a large factor. We shall postpone the consideration of the nonlinear effects to Secs. 3 and 4 and estimate here only the size effects in weak fields.

In estimating the magnitude of an anisotropic size effect as a function of the rate of surface conversion, it is convenient to begin with the case when there is no surface conversion and the thicknesses are $d_y$ $d_z \ll L$. The partial transverse currents can then be ignored throughout the sample. In weak fields $E_x$, the values of $\mathbf{E}_\perp$ and $\nabla n_\alpha$ remain almost constant throughout the sample.[6)] It follows from Eqs. (1.5) and (1.6) that

$$e_\alpha \nabla n_\alpha = e n_\alpha \varepsilon_\alpha^{-1} [\mathbf{E}_\perp + (\hat{\sigma}^\alpha_{\perp\perp})^{-1} \sigma^\alpha_{\perp x} E_x], \tag{1.7}$$

$$\mathbf{E}_\perp = -\frac{\sum_\alpha \varepsilon_\alpha^{-1} n_\alpha (\hat{\sigma}^\alpha_{\perp\perp})^{-1} \sigma^\alpha_{\perp x}}{\sum_\alpha \varepsilon_\alpha^{-1} n_\alpha} E_x, \tag{1.8}$$

where $\varepsilon_\alpha$ is governed by the condition $\hat{D}^\alpha = \varepsilon_\alpha \hat{u}^\alpha$ (in the case of nondegenerate statistics, we have $\varepsilon_\alpha = T/e$). Hence, using Eq. (1.5), we immediately obtain the formula for the current in a thin sample

$$\left.\begin{aligned} i_x = \Sigma(0) E_x, \quad \Sigma(0) = \sum_\alpha \sigma^*_\alpha, \\ \sigma^*_\alpha = \sigma^\alpha_{xx} - \sigma^\alpha_{x\perp} (\hat{\sigma}^\alpha_{\perp\perp})^{-1} \sigma^\alpha_{\perp x}. \end{aligned}\right\} \tag{1.9}$$

According to the system (1.9), each group in a thin sample makes its own contribution to the total conductivity $\Sigma(0)$ quite independently of the other groups. It must be stressed that this change in conductivity occurs when the total number of carriers in each of the groups is constant because of the diffusion contribution to the total current.

A comparison of the system (1.2) with Eqs. (1.8) and (1.9), which represent two extreme cases of thin samples (maximum and minimum rate of surface conversion, respectively) shows that the expressions for the conductivity and transverse field are quite different.

We shall now consider cubic crystals. For these crystals, we have $\sigma_{\perp x} = 0$ and it follows from Eq. (1.2) that $\Sigma(\infty) = \sigma^* = \sigma_{xx} = \sigma$, where the latter quantity is the bulk conductivity. On the other hand, the separate conductivities are $\sigma^\alpha_{\perp x} \neq 0$ and, therefore, $\Sigma(0) < \sigma$. We shall determine their ratio in the case of $n$-type germanium, whose spectrum includes four valleys, which are ellipsoids of revolution lying along [111] axes. If the $x$ axis is directed along one of the fourfold axes and the $y$ axis along the face diagonal, we find that

$$\frac{\Sigma(0)}{\Sigma(\infty)} = 1 - \frac{\sigma^1_{xy}\sigma^1_{yx}}{\sigma^1_{xx}\sigma^1_{yy}} = \left[1 + \frac{(\sigma_t - \sigma_l)^2}{4\sigma_t\sigma_l} \sin^2 2\theta\right]^{-1}, \tag{1.10}$$

where $\theta \approx 55°$ is the angle between the [100] and [111] axes, and $\sigma_l$ and $\sigma_t$ are the principal values of the conductivity for one ellipsoid. If $\sigma_l/\sigma_t \approx 0.05$ or $0.2$ (acoustic and impurity scattering, respectively[6]), we find that $\Sigma(0)/\Sigma(\infty) \approx 0.2$ and $0.5$. We shall assume that $\sigma l/\sigma_t = 0.05$.

The above discussion makes clear the two simplest manifestations of anisotropic size effects, which are the dependence of the conductivity $\Sigma$ on the thickness over distances of the order of $L$ and the appearance (even in cubic crystals!) of a transverse emf associated with the field $\mathbf{E}_\perp$.

The first to point out the phenomena which we call here anisotropic size effects was Fowler in his monograph[7] in connection with the Hall effect in an ambipolar conductor (i.e., with the effect which occurs in a length $L_r$). The interest in this size effect, usually known as the magnetoconcentration effect, was stimulated by the theoretical and experimental investigations of Welker *et al.*[8-11] A systematic theory of the size galvanothermomagnetic effects in ambipolar semiconductors was given by Pikus[12] (see also[13]). Investigations of the anisotropic size effects associated with the anisotropy not due to the magnetic field were started in[14,15]. Somewhat later, a study was made of the anisotropic size effects occurring over distances equal to the other diffusion lengths such as the intervalley length $L_v$ (electrical conductivity,[16] Hall effect,[17] magnetoresistance,[18] skin effect[19]) and the cooling length $L_\varepsilon$ (magnetoresistance[20]), which were shorter than $L_r$ in the case of semiconductors.

6)We can show that this applies for any finite rate of surface conversion provided the inequalities $d_y$, $d_z \ll L$ are satisfied sufficiently well.

### C. Main equations and boundary conditions

The currents i can be calculated normally if we know the spatial distribution of the carrier densities. We shall confine our attention to the one-dimensional case ($d_z \to \infty$), i.e., a plate of thickness $2d_y = 2d$, so that all the quantities depend exclusively on the coordinate $y$.

The dependence of $n_\alpha$ on $y$ is found from a system of equations of continuity for the currents $j^\alpha = i^\alpha/e_\alpha$:

$$\frac{\partial n_\alpha}{\partial t} + \frac{\partial j_y^\alpha}{\partial y} = \sum_{\beta \neq \alpha} (n_\alpha \tau_{\alpha\beta}^{-1} - n_\beta \tau_{\beta\alpha}^{-1}) \qquad (1.11)$$

subject to the boundary conditions on the free surfaces $y = \pm d$:

$$j_y^\alpha(\pm d) = \pm \sum_{\beta \neq \alpha} (n_\alpha^\pm s_{\alpha\beta}^\pm - n_\beta^\pm s_{\beta\alpha}^\pm), \quad n_\alpha^\pm = n_\alpha(\pm d), \qquad (1.12)$$

where we have introduced the bulk times $\tau_{\alpha\beta}$ and surface rates $s_{\alpha\beta}^\pm$ of departure from a group $\alpha$ to a group $\beta$.

We can determine all the values of $n_\alpha(y)$ and the fields $E_y(y)$ by supplementing the above system with the Poisson equation. In many important cases, it can be replaced with the quasineutrality condition (1.6) or the equivalent condition $i_y = 0$, which applies to a spatially homogeneous one-dimensional problem. Then, the rates $s_{\alpha\beta}^\pm$ are specified on the boundaries of a quasineutral region and are phenomenological parameters; we can relate them to the rates on true surfaces by solving the exact problem of surface space-charge layers.

After the elimination of $E_y(y)$, the equations have two components of the field: $E_x$ and $E_z$. The former is assumed to be given and the latter is governed by the quasi-Hall condition specifying that the total current along the $z$ direction is zero.

It must be stressed that we are confining ourselves to the one-dimensional case simply for reasons of mathematical convenience; all the principal qualitative relationships can then be followed quite fully. However, in view of the appearance of the currents along the $z$ direction, the numerical value of a size effect may sometimes be much smaller. In particular, in the case of $n$-type Ge considered at the end of Sec. 1B, we find that, in the limit $d_y \to 0$, $d_z \to \infty$, Eq. (1.10) should be replaced with

$$\frac{\Sigma(0)}{\Sigma(\infty)} = 1 - \frac{1}{2}\frac{\sigma_{xy}^1 \sigma_{yx}^1}{\sigma_{xx}^1 \sigma_{yy}^1}, \qquad (1.10a)$$

which means that, for the same parameters as before, the ratio $\sigma_l/\sigma_t$ is 0.6–0.75 (instead of 0.2–0.5).

## 2. ANISOTROPIC SIZE EFFECTS IN WEAK ELECTRIC FIELDS

We shall begin a systematic discussion of anisotropic size effects from the case of weak electric fields when the nonequilibrium carrier densities are low and proportional to $E$. In this case, the analysis is relatively simple and, to some extent, universal: the pattern is practically unaffected by the sign of carriers. On the other hand, the range of phenomena in which anisotropic size effects should be observed is fairly wide and includes the electrical conductivity, magnetoresistance, thermoelectric power, etc.

Linearization of the system (1.11)–(1.5) and elimination of $E_y(y)$ gives a system of homogeneous diffusion equations from which the first derivatives and the field $E_x$ drop out; the field occurs only in the boundary conditions [(1.12) in conjunction with (1.5)]. In the case of $\nu$ carrier groups, this system gives the $(\nu-1)$-th diffusion length $L_\varkappa$ and all the solutions are sums of the exponential functions $\exp(\pm y/L_\varkappa)$.

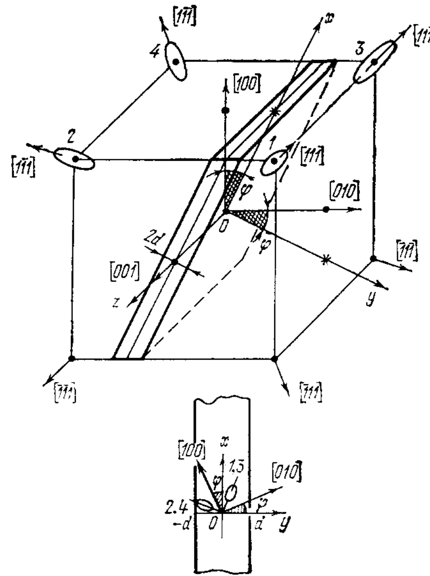


FIG. 2. Orientation of a plate relative to crystallographic axes in which a two-valley situation is established in $n$-type Ge.

### A. Intervalley redistribution of carriers

The influence of the intervalley redistribution on the electrical conductivity is considered in[16]. The results can be conveniently illustrated by the example of a semiconductor with two equivalent valleys ($\nu = 2$). It follows from the equations in Secs. 1B and 1C that, for all the anisotropic effects, the important coefficient is

$$a = a_1 - a_2, \quad a_\alpha = \frac{u_{yx}^\alpha}{u_{yy}^\alpha}. \qquad (2.1)$$

The coefficients $a_\alpha$ are a measure of the anisotropy in each of the valleys; they are one-dimensional analogs of the left-hand side of Eq. (1.4).

A realistic physical model is a plate made of $n$-type Ge and cut so that it behaves as a two-valley semiconductor. This is achieved by directing one of the fourfold axes along $z$ and the other two at an arbitrary angle $\varphi$ relative to $x$ and $y$ axes (Figs. 1 and 2).

The equations in Sec. 1C then reduce to one diffusion equation with an effective coefficient $D(\varphi)$ related to the usual bulk diffusion coefficient $D$ by

$$D(\varphi) = D(1 - a_0^2 \sin^2 2\varphi), \quad a_0 = \frac{\sigma_t - \sigma_l}{2\sigma_t + \sigma_l}. \qquad (2.2a)$$

For Ge, we find that $\sigma_l/\sigma_t \ll 1$ and $a_0 \approx 0.5$. The diffusion length $L(\varphi) = \sqrt{D(\varphi)\tau}$ also depends on $\varphi$; we also have $\tau = \tau_{\alpha\beta}/4$.[7] This diffusion length governs the depth

[7]In all those cases when there is only one relaxation mechanism, we shall drop the indices of $\tau$ and $L$.

of the layers in which intervalley redistribution takes place. The main angular dependence is contained in the anisotropic factor

$$a^2(\varphi)=a_0^2\frac{\cos^2 2\varphi}{1-a_0^2\sin^2 2\varphi}. \qquad (2.2b)$$

The degree of modulation of the conductivity is governed by the thickness $\delta=d/L(\varphi)$ and by the dimensionless surface recombination velocities $S^{\pm}(\varphi)=s^{\pm}L(\varphi)/D(\varphi)$ (in principle, the velocities $s^{\pm}$ may also include the dependence on $\varphi$):

$$\Sigma(\delta,\varphi)=\Sigma(\infty)[1-a^2(\varphi)\zeta(\delta,\varphi)]; \qquad (2.3a)$$

here, $\Sigma(\infty)=\sigma$ is the bulk electrical conductivity and

$$\zeta(\delta,\varphi)=\frac{\operatorname{th}\delta}{\delta}\frac{1+(1/2)(S^++S^-)\operatorname{cth}\delta}{1+S^+S^-+(S^++S^-)\operatorname{cth}2\delta},\quad 0\leqslant\zeta\leqslant 1. \qquad (2.3b)$$

The change in the conductivity is greatest for $\varphi=0$. Its dependence on $\delta$ for $\varphi=0$ and several values of $S^{\pm}$ is illustrated in Fig. 3. The effect disappears for $S^{\pm}\gg 1$. If only one of the recombination velocities $S^{\pm}$ is high, the effect is still large.

The field $E_y$ generates a quasi-Hall transverse emf $V_\perp=2d\overline{E}_y$, where

$$\overline{E}_y=\frac{1}{2}a_0^2\zeta(\delta,\varphi)\frac{\sin 4\varphi}{1-a_0^2\sin^2 2\varphi}E_x. \qquad (2.4)$$

In addition to $\Sigma$ and $\overline{E}_y$, direct experimental measurements can also be made of the permittivity anisotropy induced by the intervalley redistribution of free carriers. The maximum change in the surface density occurs for $S^{\pm}=0$, $\varphi=0$ and is given by

$$\frac{\Delta n(\pm d)}{n_0}=\frac{a_0E_x}{E_L}\operatorname{th}\delta,\qquad E_L=\frac{D}{uL}. \qquad (2.5)$$

The quantity $E_L$ represents the diffusion field and it sets the limit to the linear regime:

$$aE_x\ll E_L \qquad (2.6)$$

(provided $S^{\pm}\lesssim 1$).

There is one other quantity which can conveniently be studied experimentally: this is the conductivity anisotropy in the $(x, z)$ plane. It appears when the $y$ axis does not coincide with a high-symmetry direction in a crystal (i.e., with a threefold or fourfold axis). For example, if $\varphi=\pi/4$, it follows from Eqs. (2.2b) and (2.3a) that the conductivity is equal to $\sigma$, i.e., there is no size effect. However, if the current is directed in the same plane along a fourfold axis (which corresponds simply to a change of the $z$ and $x$ axes), the conductivity is

$$\Sigma=\sigma\left[1-\frac{a_0^2}{1-a_0}\zeta(\delta)\right], \qquad (2.3c)$$

where $\zeta(\delta)$ is given by Eq. (2.3b) in which $D(\varphi)\to(1-a_0)D$ and $S^{\pm}\to 4S_{12}^{\pm}=4S_{13}^{\pm}$ (Fig. 2).

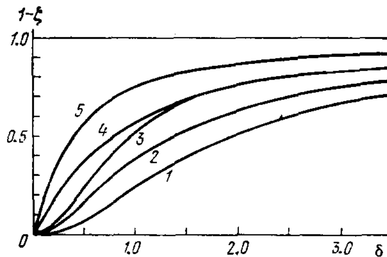


FIG. 3. Dependences of $[\Sigma(\delta)-\Sigma(0)]/a_0^2\Sigma(\infty)=1-\zeta(\delta)$ (with $\varphi=0$) $\delta$ plotted for different values of $S^{\pm}$: 1) $S^+=S^-=0$; 2) $S^+=1$, $S^-=0$; 3) $S^+=\infty$, $S^-=0$; 4) $S^+=S^-=1$; 5) $S^+=\infty$, $S^-=1$.

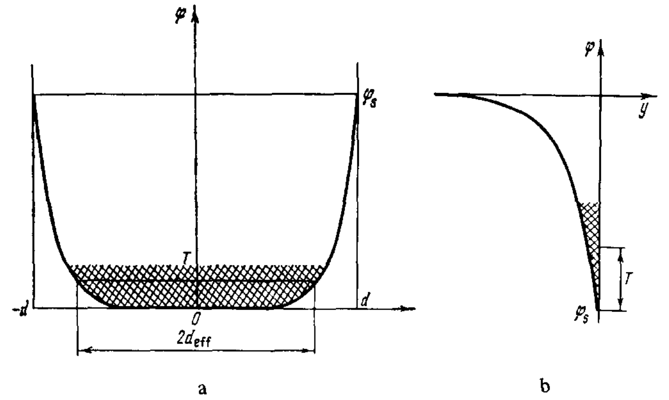


FIG. 4. Depletion (a) and accumulation (b) layers near the surface.

The latter case has an interesting feature: the conductivities of valleys 2 and 4 are not diagonal in terms of the plate axes, whereas those of valleys 1 and 3 are diagonal (we have effectively a three-valley system). Nevertheless, the field $E_y(y)$ generated by electrons in valleys 2 and 4 causes electrons from valleys 1 and 3 to participate in the intervalley redistribution: their density is highest in the central part of the plate and falls toward the edges.

The variation of the conductivity with $\varphi$ and $d$, described by Eqs. (2.2)–(2.3), does not exceed 25%. In the case described by Eq. (2.3c), the conductivity anisotropy is stronger: in the limit $d\to 0$, it may reach a factor of 2. An even greater effect is observed if anisotropic deformation transfers all the carriers in Ge to two valleys. The size-effect reduction in the conductivity may then amount to a factor of 4–5.

It should be stressed that, in the linear approximation used in the present section, the corrections to the densities are proportional to $E_x$ and, consequently, the correction to the field current is negligible. Therefore, the change in the conductivity represented by Eq. (2.3a) is entirely due to the diffusion currents.

All that we have said above applies directly only to ideal homogeneous plates in which the influence of inhomogeneous surface layers can be described by the recombination velocities $s^{\pm}$. This is possible only if the contribution of these layers to the total conductivity is negligible. Since it is unlikely that the inequality $L\ll l_D$ is satisfied by a large margin, the theory has quite rigid limits of validity.

The most favorable case is that of two depletion layers. Carriers are then concentrated in the region between these layers ($d_{eff}<d$; Fig. 4a) and $s^{\pm}$ are exponentially small. In fact, the majority of carriers is reflected from the smooth potential of the space-charge layer with momentum transfer too small for intervalley transitions and only a proportion of carriers $\sim\exp(-\varphi_s/$

$T$), where $\varphi_s$ is the band bending, reaches the real surface.

An accumulation layer in which a large number of carriers is concentrated is itself analogous to a thin sample, one of whose sides is a real surface and the other is an electrostatic potential which reflects electrons (Fig. 4b) and causes practically no intervalley scattering. For this reason, an anisotropic size effect appears in the surface layer irrespective of the actual value of $s$ on the real surface. Such an intervalley redistribution in a surface layer imposes a corresponding redistribution on the bulk electrons; the dependence $s(\varphi_s)$, which includes a sign reversal (sic!), is determined in[21]. However, if the band bending is sufficiently strong, the conductivity of a thin sample and the influence of an anisotropic size effect on the conductivity are governed by carriers in the depletion layers. The thickness of these layers, controlled by the surface charge, is then the effective thickness of a sample $d_{eff}$.

Observations of anisotropic size effects in such depletion layers are reported in[22]. An investigation was made of Ge samples with a free (112) surface. As explained above, the conductivity on such a surface should be anisotropic. Figure 5 shows the dependence of the anisotropy parameter on the band bending: we can see that this dependence appears only when the accumulation is sufficiently large. The intervalley length $L$, estimated from the thickness of the carrier localization region corresponding to the onset of the anisotropy, is $\approx 10^{-5}$ cm at 297 °K and $\approx 10^{-4}$ cm at 77 °K, in agreement with the results deduced from the acoustoelectric effect[2]; in this temperature range, the dominant effect is the phonon intervalley scattering.

### B. Redistribution of carrier energies

We shall now consider anisotropic size effects in which the individual "groups" are electrons with specific energies. In this case, an anisotropic redistribution results in the symmetric part $f_0(\varepsilon)$ of the electron distribution function $f(\mathbf{p})$ becoming dependent on the coordinate $y$.

The electronic system is characterized by the times $\tau_p$, $\tau_\varepsilon$, and $\tau_{ee}$, the last of which is the electron–electron collision time. If $\tau_p$ is governed by quasielastic scattering (see Sec. 1A), and the electron densities are relatively low, then

$$\tau_p \ll \tau_\varepsilon,\ \tau_{ee}. \tag{2.7}$$

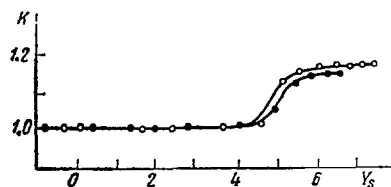


FIG. 5. Anisotropy coefficient $K=\sigma_s([\bar{1}10])/\sigma_s([111])$ of the surface conductivity $\sigma_s$ plotted as a function of the surface potential $Y_s=\varphi_s/T$ for a sample with $y \parallel [11\bar{2}]$. The black dots represent a chemically etched surface and the open circles a surface subjected to ion bombardment. [22]

If these two criteria are satisfied simultaneously, electrons of energy $\varepsilon$ form a separate group ($\varepsilon$ electrons).

We shall consider a single-valley system. The appearance of anisotropic size effects requires that $a(\varepsilon) = u_{yx}(\varepsilon)/u_{yy}(\varepsilon)$ [compare with Eqs. (1.4) and (2.1)] should differ from zero and depend on $\varepsilon$: then, different $\varepsilon$ electrons have different anisotropies. The consequences can conveniently be discussed by considering the example of transverse magnetoresistance of a semiconductor with an isotropic spectrum (H in the plane of a plate). In this case,

$$a(\varepsilon)=\omega_c\tau_p(\varepsilon), \qquad \omega_c=\frac{eH}{mc} \tag{2.8}$$

represents the tangent of the Hall angle. The classical transverse magnetoresistance appears entirely because (due to the dependence of $a$ on $\varepsilon$) the Hall field compensating the total transverse current does not compensate the partial currents (with different values of $\varepsilon$). Since anisotropic size effects influence significantly these currents, we can expect the effect to be large. This is indeed demonstrated in[20].

A special feature of this situation is that $\varepsilon$, which is the index of a group, is continuous and the transition from group to group occurs not only because of collisions but also because of the application of an external field. Therefore, instead of the system (1.11), we obtain an integrodifferential equation in terms of partial derivatives

$$\operatorname{div}\mathbf{j}-e\mathbf{E}\frac{\partial\mathbf{j}}{\partial\varepsilon}=-R[f_0] \tag{2.9a}$$

for the density of the $\varepsilon$-electron current

$$\mathbf{j}=\mathbf{j}(\varepsilon,\mathbf{r})=-g(\varepsilon)\hat{D}(\varepsilon)\left(\frac{\partial f_0}{\partial\mathbf{r}}-e\mathbf{E}\frac{\partial f_0}{\partial\varepsilon}\right); \tag{2.9b}$$

where, $R(f_0)$ is a functional describing relaxation of the function $f_0(\varepsilon)$, $g(\varepsilon)$ is the density of states in a band, and $\hat{D}(\varepsilon)$ is the tensor of the diffusion coefficients

$$D_{xx}=D_{yy}=\frac{2\varepsilon}{3m}\frac{\tau_p(\varepsilon)}{1+a^2(\varepsilon)}, \qquad D_{xy}=-D_{yx}=-\frac{2\varepsilon}{3m}\frac{a(\varepsilon)\tau_p(\varepsilon)}{1+a^2(\varepsilon)}, \tag{2.10}$$

related to the mobility $\hat{u}(\varepsilon)$ by $\hat{u}(\varepsilon) = -e\hat{D}(\varepsilon)\,\partial\ln f_0/\partial\varepsilon$. The boundary condition (1.12) becomes

$$j_y(\varepsilon,\ \pm d)=\hat{s}^{\pm}[f_0], \tag{2.11}$$

where $\hat{s}^{\pm}$ is the functional of the surface relaxation of the distribution $f_0$.

We can distinguish two limits, depending on the relationship between $\tau_\varepsilon$ and $\tau_{ee}$. If $\tau_{ee} \ll \tau_\varepsilon$, an electron temperature $T_e(y)$ is established in the electron gas, i.e.,

$$f_0(\varepsilon,\ y)\propto T_e^{-3/2}\exp\left(-\frac{\varepsilon}{T_e}\right). \tag{2.12}$$

The temperature $T_e(y)$ is given by the equation for the electronic thermal conductivity; it is established in a distance $L_{ee} \sim \sqrt{D\tau_{ee}}$ and relaxes in a cooling length $L_\varepsilon \sim \sqrt{D\tau_\varepsilon}$. However, if $\tau_{ee} \gg \tau_\varepsilon$, the electron–electron collisions are unimportant; $f_0$ is then non-Maxwellian and relaxes in a distance $L_\varepsilon$.

It is convenient to begin with $\tau_\varepsilon \ll \tau_{ee}$, discussed in [23] in the specific case of acoustic scattering, and to rep-

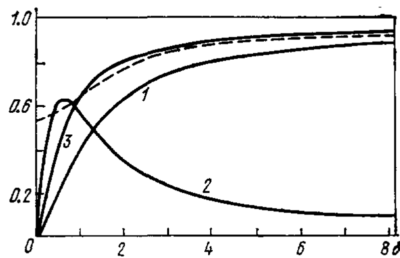


FIG. 6. Size coefficients in the formula (2.13) for some limiting cases on surfaces[23]: 1) $1-\zeta_1(\delta)$ for $\hat{s}^+=\hat{s}^-=0$; 2) $\zeta_2(\delta)$ for $\hat{s}^-=0$, $\hat{s}^+=\infty$; 3) $1-\zeta_1(\delta)$ for $\hat{s}^-=0$, $\hat{s}^+=\infty$. The dependence $1-\zeta_2(\delta)$ for $\hat{s}^-=\hat{s}^+=\infty$ is practically identical with curve 1 and for $\hat{s}^-=0$, $\hat{s}^+=\infty$ with curve 3. The dashed line is function $1-\zeta_1(\delta)$ corresponding to $s_\varepsilon^\pm=0$, obtained in the temperature approximation for the scattering of electrons by acoustic phonons.[20] If $s^\pm=\infty$, $f_0^\pm$ has the equilibrium value on the corresponding surface.

resent the weak-field conductivity in the form[24]

$$\Sigma(\delta)=\sigma\left[1-\left(\frac{H}{H_0}\right)^2(1-\zeta_1(\delta))-\left(\frac{E_x}{E_0}\right)^2(1-\zeta_2(\delta))+b_1\frac{E_xH}{E_0H_0}\zeta_3(\delta)\right],\quad b_1\approx 0.275; \tag{2.13}$$

here, the second term in the brackets describes the magnetoresistance, the third the nonohmic behavior, and the last term in the mixed effect; $E_0\sim T/eL_\varepsilon$ and $H_0\sim mc/e\tau_p$ are the characteristic electric and magnetic fields. The functions $\zeta_i(\delta)$ describe the size effect: $\zeta_1$ and $\zeta_2$ decrease monotonically from 1 to 0 with increasing $\delta$ and $\zeta_3(0)=\zeta_3(\infty)=0$; $|\zeta_3|$ passes through a maximum at $\delta\sim 1$ and differs from zero only if $\hat{s}^+\neq\hat{s}^-$. If $\hat{s}^+=\hat{s}^-=0$, only $\zeta_1$ differs from zero and the size effect is exhibited solely by the magnetoresistance. If $\hat{s}^+=\hat{s}^-=\infty$, only $\zeta_2$ is retained. For $\hat{s}^+=0$, $\hat{s}^-\to\infty$, we find that $\zeta_i\neq 0$. The explicit form of the functions $\zeta_i(\delta)$ depends on the functionals $\hat{s}^\pm$, which are not known. Figure 6 shows the form of the functions $\zeta_i(\delta)$ for certain limiting conditions on the surface.

It is clear from Fig. 6 that, if $d\to 0$ and $\hat{s}^\pm\neq\infty$, the transverse magnetoresistance vanishes.[8)] This result is general and is also valid in strong (but not quantizing) magnetic fields. It is self-evident in the $\hat{s}^+=\hat{s}^-=0$ case the transverse currents (responsible for the transverse magnetoresistance) vanish on the surface and, therefore (for $d\ll L_\varepsilon$!), throughout the sample. If $s^\pm\neq 0$, the result is still valid since the dimensionless surface relaxation rate in a thin plate is now $s_\varepsilon d/D$ (here, $s_\varepsilon$ is the characteristic rate corresponding to the operators $\hat{s}^\pm$), which vanishes in the limit $d\to 0$.

In strong magnetic fields, the value of $D$ decreases as $H^{-2}$, in accordance with Eq. (2.10). Consequently, we have $L_\varepsilon\propto H^{-1}$ and the ratio $d/L_\varepsilon$ increases proportionally to $H$; therefore, the anisotropic size effect weakens with increasing $H$. This is illustrated in Fig. 7. If H is normal to the plane of the plate, the size effect should

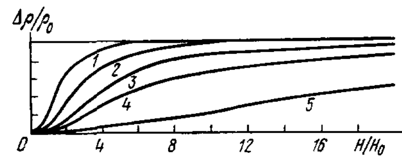


FIG. 7. Schematic representation of the dependences of the magnetoresistance on a magnetic field (H ∥ z) for samples of different thickness: 1) $d\gg L_\varepsilon$; 2) $d>L_\varepsilon$; 3) $d\sim L_\varepsilon$; 4) $d<L_\varepsilon$; 5) $d\ll L_\varepsilon$; $L_\varepsilon$ is the diffusion length in $H=0$.

not be observed; therefore, the transverse magnetoresistance of a thin sample should depend quite strongly on the orientation of H.

If $\tau_\varepsilon\gg\tau_{ee}$, the theory in[20,24,23] simplifies considerably because the temperature approximation can be applied if $d>L_{ee}$, and new details appear in the physical picture. These details are associated with the existence of an intermediate range of thicknesses $L_{ee}\lesssim d\ll L_\varepsilon$, in which electrons become thermalized and the total transverse electron energy flux does not change significantly. Therefore, the size-induced change in the transverse magnetoresistance occurs in two stages: when the thickness of the sample is reduced, we find that, in the range $d\sim L_\varepsilon$, the transverse magnetoresistance falls from its bulk value $(\Delta\rho/\rho)_\infty$ to an intermediate value $(\Delta\rho/\rho)_{L_{ee}}$ corresponding to the lower limit of validity of the temperature approximation ($L_{ee}\ll d\ll L_\varepsilon$) (Fig. 8). A further reduction in $\Delta\rho/\rho$ to zero occurs in the range of thicknesses $d\sim L_{ee}$. The value of the ratio $(\Delta\rho)_{L_{ee}}/(\Delta\rho)_\infty$ depends strongly on the scattering mechanism.[20] For the deformation acoustic scattering, this ratio is 0.54, whereas, for other mechanisms, it is much smaller than unity (i.e., practically the whole of the fall of $\Delta\rho/\rho$ occurs in the range corresponding to the temperature approximation).

The criterion of weak redistribution is $E\ll E_{L_\varepsilon}$, where $E_{L_\varepsilon}=T/eL_\varepsilon\sim E_0$ is the diffusion field active in the energy redistribution. However, this criterion is the condition for weak heating. Therefore, strong heating may be accompanied by a strong redistribution of $T_e$ in a sample.[26]

Anisotropic size effects also appear in other transport phenomena in which the transverse currents are important, for example, in the longitudinal Nernst–Ettingshausen effect (the change in the thermoelectric power in a transverse magnetic field). The contribution of the drag of electrons by phonons may reverse the sign of the magnetothermoelectric power and, in the same temperature range, the size dependences may be monotonic

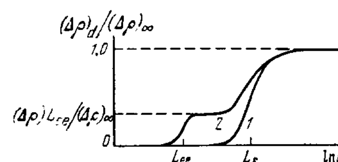


FIG. 8. Size dependence of the transverse magnetoresistance in two limiting cases: 1) $L_{ee}\gg L_\varepsilon$; 2) $L_{ee}\ll L$. In case 2, the size-induced change occurs in two stages.

---

8)We shall not consider the range of small thicknesses $d\lesssim l_p$ when the magnetoresistance, in the case of diffuse scattering, is of different origin.[25]

and exhibit sign reversal.[27] Several other effects are described in the review[28].

### C. Combined mechanism of anisotropic size effects in magnetoresistance of semiconductors

The transverse magnetoresistance in one-valley semiconductors is associated with the transverse currents of the $\varepsilon$ electrons. In many-valley semiconductors, there is an additional mechanism associated with the transverse currents of various $\alpha$ electrons; therefore, the transverse magnetoresistance does not disappear even for $\tau_p(\varepsilon)=\text{const}$. If $L_v \gg L_\varepsilon$, the size-induced change in the transverse magnetoresistance, due to the intervalley mechanism, appears throughout the range $d \lesssim L_v$, and that due to the energy mechanism only for $d \lesssim L_\varepsilon$.

Then, if $d \gg L_\varepsilon$, the theory is exactly the same as in Sec. 2A. The only difference is that the tensors $u_{ij}^\alpha$ have antisymmetric parts. Therefore, the transverse magnetoresistance differs from zero also for the orientations of a crystal for which there is no size effect in the electrical conductivity.

Galvanomagnetic intervalley phenomena in Ge are considered in[29] in the configuration shown in Sec. 2A. If $\mathbf{H} \parallel y$, the Hall field $E_z$ has a strong size dependence: when $d$ is varied, the ratio $E_z/E_x$ changes by a factor of 4 [i.e., much more than the conductivity—compare with Eq. (2.3a)]. If $\varphi \neq 0$ or $\pi/4$, a longitudinal Hall effect appears (this effect is not observed in bulk samples). An unexpected feature is the weak dependence of the size-induced transverse magnetoresistance on the angle $\varphi$ [in contrast to the size-induced dependence of the conductivity—compare with Eqs. (2.2) and (2.3)] and on the direction of H in the $(y, z)$ plane. When $d$ is reduced, the transverse magnetoresistance remains finite provided $\tau$ depends on $\varepsilon$; in the acoustic scattering case, it falls by a factor of about 2. A further fall to zero occurs in the range $d \lesssim L_\varepsilon$. In this range, the two mechanisms of the transverse magnetoresistance are activated in turn (like the $L_\varepsilon$ and $L_{ee}$ mechanisms in Sec. 2B). A calculation for the three-valley case of $n$-type Si is given in[30].

Clearly, the inequality $L_v \gg L_\varepsilon$ is never very strong. We can easily find the situations in which the converse inequality can be expected (for example, a heavily doped semiconductor). Therefore, the case $L_v \sim L_\varepsilon$ is important; in this case, the mechanism of the anisotropic size effects is of the combined type. Since the dependences $a_\alpha(\varepsilon)$ vary from valley to valley, the departure from an equilibrium energy distribution occurs under different circumstances in each valley and this gives rise to an additional intervalley redistribution mechanism (similar to that in heating fields[31]). Similarly, the unequal occupancies of the valleys generate carrier currents and, consequently, energy fluxes between the valleys.

The actual result depends on the scattering mechanism. In the impurity intervalley scattering case, the dependence $\tau_v(\varepsilon)$ for the mechanisms with virtual or real electron capture by donors[2] is a rising function of $\varepsilon$; therefore, slow electrons participate mainly in intervalley transitions and these transitions heat the more heavily populated valley and cool the less populated one. In heating fields, this situation corresponds to the anomalous Sasaki effect.[32] In the phonon intervalley scattering, the opposite result should be obtained because $\tau_v(\varepsilon)$ falls strongly in the range $\varepsilon \gtrsim \omega_{ph}$.

In this situation, the intervalley redistribution produces a nonequilibrium energy distribution not only in the transverse magnetoresistance but also in the size-affected electrical conductivity.[33]

The mutual influence of the two mechanisms becomes weaker at high carrier densities because of the exchange of energy between the valleys resulting from the electron–electron collisions. It is shown in[34] that, in the common temperature approximation, the two mechanisms can be separated in weak and strong fields $H$ (and for an arbitrary configuration $\mathbf{H} \parallel z$ in Fig. 2), and the contributions of these mechanisms to the magnetoresistance are additive.

### D. Surface relaxation

We may assume that the surface rates (velocities) of intervalley scattering $s_v$ and cooling $s_\varepsilon$ are—like the thoroughly investigated surface recombination velocity $s_r$—structure-sensitive quantities and depend strongly on the state of the surface. It is well known[9)] that $s_r$ of Ge can be varied within the range $10^2$–$10^6$ cm/sec by a suitable surface treatment and field-induced band bending.

In the absence of surface band bending, it follows from general considerations that $s_v$ should be large and $s_\varepsilon$ should be much smaller. In fact, $s_\varepsilon$ should be related to the inelastic processes. Conversely, $s_v$ may be due to elastic scattering accompanied by the transfer of large momenta to surface imperfections on the atomic scale. If the concentration of such imperfections is high, the value of $s_v$ should be comparable with the average velocity of the "boundary" flux $\bar{v}/4$. In the phenomenological theory, the rates $s_v$, comparable with $v$, should be regarded as $s_v=\infty$. The rate $s_v$, may be considerably smaller for atomically perfect surfaces and in the presence of depletion layers[35] (see Sec. 2A). In this case, we clearly have $s_v \lesssim (1/4)\bar{v}\exp(-\varphi_s/T)$. A slight band bending $\varphi_s \sim 3T$ ensures the necessary reduction in $s_v$.

The occurrence of surface energy relaxation should[36] reduce considerably the electron heating in layers with $d \lesssim L_\varepsilon$ and alter the conductivity (and all the galvanomagnetic coefficients[28,37]) in heating fields so that the conductivity becomes size-sensitive.

This effect was observed in $n$-type Si[38–40] and in $p$-type Ge[41] at 77 °K. The experiments on $p$-type Ge were carried out on plates whose thickness was varied by grinding and etching, whereas the experiments on $n$-type Si were carried out using surface channels of a width controlled by the nonequlibrium depletion method.[42] A strong size effect in the electrical conductiv-

[9)] See, for example, §18 in[151].

ity, exhibited by both $n$-type Si in the absence of band bending[38,39] and Ge,[41] corresponded to an unexpectedly high value of $s_\varepsilon$, which was of the order of the thermal velocity $\bar{v}$. In the case of $n$-type Si with depletion layers,[40] the dependence of the electrical conductivity on the size was not observed in the range $E < 500$ V/cm but appeared fairly abruptly in fields $E \gtrsim 500$ V/cm. These results demonstrated the efficiency of the suppression of $s_\varepsilon$ by depletion layers and the possibility of overcoming the barriers by strongly heated electrons. The high values of $s_\varepsilon$ reported in[38,39,41] can be explained in a natural manner by a two-stage relaxation mechanism when energy is first transferred to electrons localized at the surface levels (and characterized by a quasicontinuous spectrum) followed by the transfer of energy to the lattice.

This subsection can be summarized as follows: the establishment of a depletion layer on at least one surface should facilitate observations of anisotropic size effects over distances $L_v$ and $L_\varepsilon$.

## E. Experimental investigations of size anisotropy of magnetoresistance

A special dependence of the transverse magnetoresistance on the orientation of H in thin samples was reported in several papers.[43–49] In all cases, use was made of samples known to exhibit a strong dependence of the conductivity on $y$. This inhomogeneity could of itself give rise to an anisotropy of the transverse magnetroresistance, i.e., it could give rise to a dependence of this magnetoresistance on the orientation of H in the $(y, z)$ plane. However, it was concluded in the investigations of $p$-type Ge[45–48] and $n$-type GaAs[49] that inhomogeneities could not account for the whole of the observed effect and, therefore, the size effect over distances $L_\varepsilon$ was invoked (see Sec. 2B). The transverse magnetoresistance anisotropy exhibited by macroscopically homogeneous samples of $p$-type Ge was also attributed to the size effect[50]; however, the measurements in[50] were carried out in strong magnetic fields which enhanced the importance of small random inhomogeneities.[51]

We shall now consider in greater detail the results reported in[52] where the homogeneity of $n$-type Si plates, which were $2d = 40–700$ $\mu$ thick, was checked specially and moderate magnetic fields were used. The

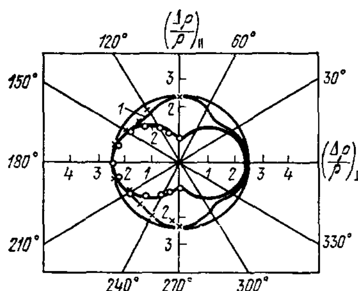


FIG. 9. Dependence of the transverse magnetoresistance on the angle between **H** and the $y$ axis in thick and thin samples[52]: 1) $2d = 700$ $\mu$; 2) $2d = 40$ $\mu$.

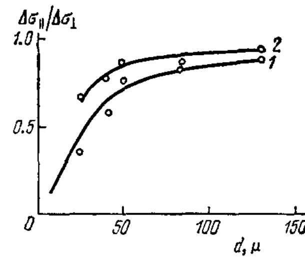


FIG. 10. Dependence of the ratio of the magnetoresistances for **H**$\parallel z$ ($\Delta\sigma_\parallel$) and **H**$\parallel y$ ($\Delta\sigma_\perp$) on the half-thickness of a sample at $T = 25$ °K[52]: 1) $uH/c = 0.5$; 2) $uH/c = 1$; the circles are the experimental values and the curves are the theoretical dependences.

plate axes were oriented along fourfold crystallographic axes so that the anomalous size effect was not exhibited by the conductivity. The rates of surface relaxation were reduced by establishing depletion layers on the surface. Figure 9 shows the angular distributions of the transverse magnetoresistance in samples of two thicknesses: it is clear that the distribution for a thick sample has a fourfold axis, whereas that for a thin sample has only a twofold axis. Figure 10 shows the thickness dependences of the ratios of the magnetoresistances obtained for H $\parallel z$ and H $\parallel y$ for two values of $H$. These results are used in[52] to determine the characteristic relaxation length $L \approx 15$ $\mu$ (at $T = 25$ °K), which is in satisfactory agreement with the value of $L_\varepsilon$, calculated by the same authors on the basis of the results reported in[38]. The effect is treated in[53] as of the combined type (see Sec. 2C) occurring over distances $L_\varepsilon$ and $L_v$, which—as indicated by indirect estimates—are of the same order of magnitude[10)]; it should be noted that, in the phonon scattering range, we always have $L_v \gtrsim L_\varepsilon$. The experimental dependences of the effect on $T$ (in the range 20–160 °K) and $H$ are in agreement with this interpretation.

We shall now state the conclusions. Experimental investigations of anisotropic size effects over distances equal to the intervalley length $L_v$ and cooling length $L_\varepsilon$ are difficult primarily because, in the case of semiconductors, these lengths are short. A quantitative theoretical interpretation of the results is also complicated by the fact that, although the characteristic lengths $L_\varepsilon$ and $L_v$ are "literally" independent and, in principle, can differ considerably, in real situations the difference between them is small and, therefore, we may expect to observe the combined mechanism. Judging by all the evidence, this is the effect observed in $n$-type Si.

## F. Intervalley redistribution in semimetals

Semimetals such as Bi (see, for example,[54,55]) have many-valley electron spectra and, therefore, they can exhibit intervalley redistribution. However, the numerical values of certain parameters of semimetals are such that it is desirable not to confine the treatment to the phenomenological theory but to extend it to the range

[10)]Recent independent measurements of $\tau_v$ of Si gave $10^{-8}$–$10^{-9}$ sec.[158]

of thicknesses $d \sim l_p$ on the basis of a solution of the transport equation.

The point is that, in contrast to semiconductors whose lengths $l_p$ are short ($l_p < 10^{-4}$ cm), the value of $l_p$ for Bi reaches 0.3 mm and such thicknesses are encountered in studies of the size effect (see next subsection). On the other hand, the ratio $L_v/l_p$ does not exceed 10 even for the best samples. Moreover, when the thickness is increased, the size effects decrease proportionally to $d^{-1}$, i.e., they decrease slowly so that there may be an overlap between the regions in which the size effects associated with different characteristic lengths are observed. Therefore, it is desirable to obtain equations valid for all the thicknesses; this naturally results in the loss of the advantages of the phenomological approach because certain assumptions must now be made in advance about the energy spectrum and nature of the relaxation processes.

This theory was developed for a special situation in[56] and for the general case in[57]. We shall confine ourselves to a model demonstrating the general approach. If we assume that $f_\alpha = f_0(\varepsilon - \varepsilon_F) + \varphi_\alpha\, \partial f_0/\partial_\varepsilon$, we find that, for $\tau_v \gg \tau_p$, the transport equations for separate electron valleys (derived in the approximation of a scalar relaxation time) are:

$$v_y \frac{\partial \varphi_\alpha}{\partial y} - e\mathbf{E}\mathbf{v} + \frac{\varphi_\alpha - \bar{\varphi}_\alpha(y)}{\tau_p} + \sum_{\alpha' \neq \alpha} \frac{\varphi_\alpha - \bar{\varphi}_{\alpha'}(y)}{\tau_v} = 0. \tag{2.14}$$

The bar above a quantity denotes averaging in a given valley. The quantities $\bar{\varphi}_\alpha(y)$ are corrections to the chemical potentials of the individual valleys. In the case of a system of equivalent electron ellipsoids, the quasineutrality conditions are

$$\sum_\alpha \bar{\varphi}_\alpha(y) = 0. \tag{2.15}$$

If we assume that the intravalley scattering is diffuse (its probability is $w_{\alpha\alpha}$) and the intervalley is described by the probabilities $w_{\alpha\alpha'}(\alpha' \neq \alpha)$, the condition of continuity of the fluxes (currents) on the $y = -d$ surface is

$$\varphi_\alpha^{>}(-d)\,\overline{(v_y)_\alpha^{>}} + \sum_{\alpha'} w_{\alpha'\alpha} \overline{v_y \varphi_{\alpha'}^{<}(-d, \mathbf{v})} = 0, \quad \sum_{\alpha'} w_{\alpha'\alpha} = 1 \tag{2.16}$$

and there is a corresponding condition for the $y = d$ surface.[57,58] The function $\varphi^{\gtrless}$ refers to the $v_y \gtrless 0$ cases; similarly, the superscripts $\gtrless$ of any other quantity indicate that they differ from zero only if $v_y \gtrless 0$. The subscript identifies the valley for which the averaging is carried out.

If we consider $\bar{\varphi}_\alpha(y)$ and $\mathbf{E}(y)$ in Eq. (2.14) to be known functions, the solution of this equation is of the Fuchs type[1]:

$$\varphi_\alpha^{\gtrless}(y, \mathbf{v}) = \beta\bar{\varphi}_\alpha(y) + \Big[(\varphi_\alpha^{\gtrless}(\mp d) - \beta\bar{\varphi}_\alpha(\mp d)) \exp\Big(-\frac{y \pm d}{v_y \tau}\Big) + \frac{1}{v_y} \int_{\mp d}^{y} dy' e(\mathbf{v}\mathbf{E}_\alpha(y')) \exp\Big(\frac{y' - y}{v_y \tau}\Big)\Big], \tag{2.17}$$

where

$$\beta = \tau\Big(\frac{1}{\tau_p} - \frac{1}{\tau_v}\Big), \quad \frac{1}{\tau} = \frac{1}{\tau_p} + \frac{\nu - 1}{\tau_v}, \tag{2.18}$$

and the quasifields are

$$\mathbf{E}_\alpha(y) = \Big(E_x,\ E_y - \frac{\beta}{e}\frac{d\bar{\varphi}_\alpha}{dy},\ E_z\Big). \tag{2.19}$$

Equation (2.16) gives $2\nu$ constants of integration $\varphi_\alpha^{\gtrless}(\mp d)$. The quasifields $\mathbf{E}_\alpha(y)$ are found by making the solutions of Eq. (2.17) self-consistent by a procedure involving averaging over the velocities (rates). In the case of the quadratic dispersion law $\varepsilon_\alpha(\mathbf{p})$:

$$(\varphi_\alpha^{<}(d) - \beta\bar{\varphi}_\alpha(d))\,\overline{(e^{(y-d)/v_y\tau})_\alpha^{>}} + (\varphi_\alpha^{>}(-d)) - \beta\bar{\varphi}_\alpha(-d))\,\overline{(e^{-(y+d)/v_y\tau})_\alpha^{>}} - \int_{-d}^{d} dy' \operatorname{sign}(y' - y)\, e\mathscr{E}_\alpha(y')\,\overline{(e^{-(|y-y'|)/v_y\tau})_\alpha^{>}} = (1 - \beta)\bar{\varphi}_\alpha(y), \tag{2.20}$$

where

$$\mathscr{E}_\alpha(y) = \sum_i E_{\alpha i}(y) \frac{\varepsilon_{iy}^\alpha}{\varepsilon_{yy}^\alpha}, \quad \varepsilon_\alpha(\mathbf{p}) = \frac{1}{2} \sum_{ij} \varepsilon_{ij}^\alpha p_i p_j. \tag{2.21}$$

The equations (2.20) together with the conditions (2.15) can be used, in principle, to find all the values of $\bar{\varphi}_\alpha(y)$ and the field $\mathbf{E}(y)$.

These equations are solved analytically (for limiting situations) or numerically. Analytic singularities of the solutions can be separated by differentiating Eq. (2.20). We can see that $\mathscr{E}_\alpha(y)$ contains terms of the type $\{(1/v_y) \times \exp[(z - d)/v_y\tau]\}_\alpha^{>}$, which give rise to contributions proportional to $\ln[(d^2 - y^2)/l_p^2]$. Therefore, the values of $E_y$ and $d\bar{\varphi}_\alpha/dy$ diverge logarithmically at the edges.

We shall now consider the conditions in a surface layer. In the case of Bi, we have $l_D \sim 10^{-6}$ cm and the inequality $l_D \ll l_p$ is well satisfied, i.e., the electron motion in the surface layer is ballistic. Since $\varepsilon_F \sim 10^{-2}$ eV, a surface field $E_s \sim 10^4$–$10^5$ V/cm is sufficient to ensure that $|\varphi_s| \gtrsim \varepsilon_F$. Then, depending on the sign of $\varphi_s$, the potential is repulsive for carriers of one sign (electrons or holes). These carriers escape to the surface only if their velocity lies within an "attainability cone," namely, if $|v_y| > (2\varepsilon_{yy}|\varphi_s|)^{1/2}$. The considerations put forward in Secs. 2A and 2D demonstrate the intervalley scattering should be experienced by carriers within the "attainability cone" [ensuring that $s_{\alpha\alpha'} \sim (1/4)vw_{\alpha\alpha'}$], whereas carriers outisde this cone are scattered inside the valley and the scattering is largely [57] specular.[11] This mechanism can simulate the diffuse scattering "cutoff" discussed in the case of size effects in[59].

We shall now list the principal conclusions which follow from an analysis and solution of the above system.

All the quantities have two characteristic lengths $l_p$ and $L_v$. In the case of samples with $d \gg l_p$, the results are the same as those deduced from the phenomenological theory (compare with Sec. 2A), except that, in quasineutral surface layers $\sim l_p$ thick, the fields and carrier densities have singular terms so that $E_y \propto E_x d \ln\bar{\varphi}_\alpha/dy \propto E_x w_{\alpha\alpha'} \ln[(d^2 - y^2)/l_p^2]$[12]). Here, we

---

[11])The influence of a surface barrier on carrier reflection was established experimentally in recent investigations[156a,159], where a strong angular dependence of $q$ was established directly (for electrons in Bi) and a considerable difference between the values of $q$ for electrons and holes was found for Sb.

[12])These terms should be manifested in the effects which receive a considerable contribution of carriers moving in a layer $\lesssim l_p$ thick near the surface; for example, they may be manifested in electromagnetic generation of sound (Sec. 5b) of wavelength $\lambda \sim l_p$.

have probabilities $w_{\alpha\alpha'}$ with $\alpha \neq \alpha$ and, therefore, these singular terms disappear if the intervalley scattering is suppressed (for example, if the bands are bent so that only holes with a one-valley spectrum are present on the surface). The conductivity $\Sigma(d)$ in plates of this kind is governed only by the intervalley scattering rate, is independent of the degree of reflection specularity $q$, and is described by the expressions obtained in Sec. 2A, i.e., the conductivity exhibits a plateau in the range $l_p \ll d \ll L_v$.

In the case of samples with $d \lesssim l_p$, the analytic behavior of $\Sigma(d)$ is influenced greatly by the degree of diffuseness of the surface scattering and the characteristic length is naturally $l_p$. However, the amplitude of the change in $\Sigma(d)$ in this range is a function of all the probabilities $\omega_{\alpha\alpha'}$. If the bands are not bent, all the carriers reach the surface and the asymptotic effective range in thin plates $[d \ll l(1-q)]$ is

$$l^* \sim \frac{d}{1-q} \ln\left[\frac{l_p(1-q)}{d}\right]$$

(by analogy with[11]). However, if the bands are bent, electrons moving outside the "attainability cone" are scattered specularly and, in the limit $d \to 0$, they make a finite contribution to $\Sigma$; therefore, $\Sigma(d)$ tends to a finite limit for $d \to 0$. If $q=1$ (specular scattering!) applies to all carriers, the conductivity is constant over distances $d \sim l_p$ and the plateau in the range $d \ll L_v$ extends to $d \sim l_D \ll l_p'$. If $d \ll l_p$, the logarithmic terms in $E_y$ and $d\varphi_\alpha/dy$ include a small parameter $d/l_p$; according to the numerical calculations reported in[60], $E_y(y)$ and $d\bar{\varphi}_\alpha/dy$ then vary only weakly within a sample. If all the probabilities are $w_{\alpha\alpha'}=0$ for $\alpha \neq \alpha'$, the transverse carrier currents of all groups balance out and both $E_y$ and $d\bar{\varphi}_\alpha/dy$ are constant.[56]

The general nature of the theoretical dependences $\Sigma(d)$ can be judged from Fig. 11, which applies to Bi. If $s_v=0$ and either electrons ($q_n=1$) or holes ($q_p=1$) are scattered specularly, three plateaus (curves 2 and 3 in Fig. 11a) are observed; if $q_n=q_p=1$, two plateaus with a transition region at $d \sim L_v$ can be found. If $s_v$ is large, the size effect is manifested mainly for $d \sim l_p$ and the plateau in the range $d \ll l_p$ appears only if $q_p=1$ for holes.

It should be stressed that a consistent solution of Eqs.

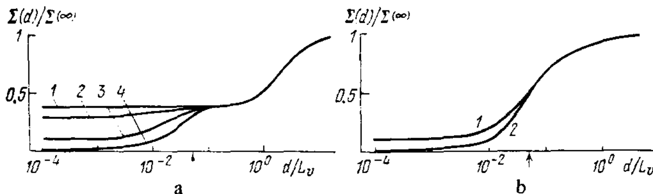


FIG. 11. Theoretical curves for the size effect in the electrical conductivity of Bi. The trigonal axis is $C_3 \| z$ and the binary axis is $C_2 \| z$ and the binary axis is $C_2 \| y$. In this geometry, there is no redistribution of holes and electrons in one valley. The carrier mobilities are taken from[69]; $L_v/L_p=10$. a) $s_v=0$: 1) $q_n=q_p=1$; 2) $q_n=1$, $q_p=0$; 3) $q_n=0$, $q_p=1$; 4) $q_n=q_p=0$. b) $s_v=10$: 1) $q_n=0$, $q_p=1$; 2) $q_n=q_p=0$; the arrow identifies the value $2d=l_p$.

(2.20) and (2.16) is essential if correct results are desired. In the early papers, the transport equation was applied to the size effect in many-valley systems[59,61–63] and the self-consistency conditions were not satisfied; a basically incorrect result was obtained in[62,63], where a prediction was made of the existence, for specular scattering ($q=1$), of the size effect in a distance $l_p$ in the case of ellipsoidal valleys (compare curve 1 in Fig. 11a and the results reported in[56,64]).

We shall illustrate the influence of a magnetic field in the $\mathbf{H} \| z$ geometry. Since the Larmor radius is $r_L = v/\omega_c \ll l_p$, it governs the size of the region of nonlocal action in the calculation of the conductivity. If $r_L \ll d$, the phenomenological theory applies throughout the plate. In semimetals, the electron and hole densities are equal ($n=p$) and the conductivity of the bulk samples is $\Sigma \propto H^{-2}$ (see[65], §27) due to the disappearance of the Hall field in a lower order of $a^{-1} = r_L/l_p$ [compare with Eq. (2.8)]. In a strong field, the diffusion length decreases: $L_v(H) \sim L_v/a \ll L_v$. The conductivity of thin plates with $r_L \ll d \ll L_v(H)$ can be found from Eq. (1.9). Allowing that $\sigma_{xy} = -\sigma_{yx} \sim \sigma/a$ and $\sigma_{yy} = \sigma_{xx} \sim \sigma/a^2$ [see, for example, Eq. (2.10)], we obtain $\sigma_\alpha^* \sim \sigma$, which is identical with the conductivity in $H=0$. This is due to the existence of transverse gradients which act as the effective Hall field and each group of carriers behaves independently as in a unipolar metal. In a bulk sample of thickness $d \gg L_v(H)$, the surface layers of thickness $\sim L_v(H)$ have a higher conductivity. Therefore, the distribution of the current is similar to that in the static skin effect (see[58] and[65], §29), except for the difference that a region of higher conductivity extends not to $r_L$ but to $L_v(H) \sim r_L(\tau_v/\tau_p)^{1/2} \gg r_L$. If $s_v \lesssim L_v/a\tau_v$, the contribution of layers of this thickness to the conductivity $\Sigma(d)$ is $\sim \sigma L_v/ad$. If $s_v \gtrsim L_v/a\tau_v$, the contribution of such layers to the conductivity is $\sim \sigma D/a^2 d s_v$.[12,66,67] The size effect appears when the contribution to $\Sigma(d)$ of the surface layers becomes comparable with $\sigma_{xx} \sim \sigma/a^2$. In the two ranges of the values of $s_v$ identified above, this corresponds to $d \sim aL_v$ and $d \sim D/s_v \sim l_p v/s_v$, respectively.

Thus, in a strong magnetic field, there are three characteristic lengths at which the size effect should appear: $r_L$, $L_v(H)$, and $aL_v$ or $D/s_v$. The last two lengths may exceed considerably $L_v(H)$.

A description of the effects occurring at distances $\sim r_L$ is given in[67] in terms of the transport equation approach similar to that used in[57]. If $q \neq 1$ at the boundaries, both $E_y(y)$ and $d\bar{\varphi}_\alpha/dy$ have singularities of the $(r_L/(d-|y|))^{1/2}$, type, which influence considerably the Hall coefficient (in the $\mathbf{H} \| z$ configuration). Since the magnetic field bends the trajectories, the glancing electrons enter the "attainability cone" and, consequently, the conductivity plateau disappears for small thicknesses in the range $r_H \lesssim d$.

## G. Size effect in electrical conductivity of Bi

The interest in the size effect in the electrical conductivity of Bi has been stimulated by the discovery[68] of the saturation of $\Sigma(d)$ in the range of small thicknesses $d \lesssim 1$ mm. The results reported in that paper are plotted in Fig. 12. They were interpreted on the basis of[63] as

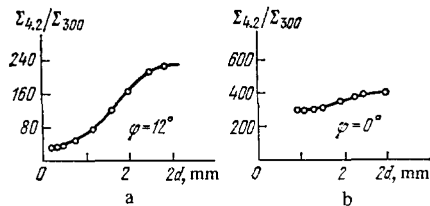


FIG. 12. Dependences of the electrical conductivity of Bi on its thickness at 4.2 °K.[68] Orientation $C_3 \| z$, $\varphi$ is the angle between $C_2$ and $x$.

the size effect in a distance $l_p$ resulting from the specular surface scattering in systems with anisotropic spectra. We have shown above (Sec. 2F) that such an effect does not occur. Moreover, the cited interpretation is in conflict with some experimental results: the distance $l_p \approx 1$ mm deduced from the size effect is considerably greater than that obtained from the mobility ($l_p \approx 0.1$–$0.4$ mm at 4.2 °K, according to[69]; see also[70]). For Bi at 4 °K, we have $\tau_v/\tau_p \sim 30$[71]; this ratio was determined for $\tau_r$ because the intervalley scattering and recombination in Bi involved practically the same momentum transfer and we might expect that $\tau_v \approx \tau_r$. It is suggested in[35] that the observations can be attributed to the anisotropic size effect in a distance $L_v$. In the case of thin plates ($d \ll L_v$), and for $S \ll 1$, the angular dependence $\Sigma(d, \varphi)$ is exactly the same as that obtained in[63] for $d \ll l_p$; therefore, the qualitative agreement with the theory of[63] obtained in[68] on the basis of an analysis of the dependence of $\Sigma$ on $\varphi$ applies equally well to the interpretation based on the anisotropic size effect. This interpretation explains why the value of $\Sigma$ reported for thin samples in[68] was finite when a special surface treatment destroyed the scattering specularity; this was a natural consequence of $s_v$ being small.

Subsequently, similar experiments were carried out by several authors on plates, wedge-shaped samples, etc. Typical experimental curves are plotted in Fig. 13. We can see that, in all cases, the characteristic length is ~2 mm. Curves 2 and 4 exhibit an additional fall in the range $d \sim 0.5$ mm, which may be due to the size effect in a distance $l_p$. This tendency also appears in the results reported in[70] where it is reported that the mobility of some samples saturates again in the range

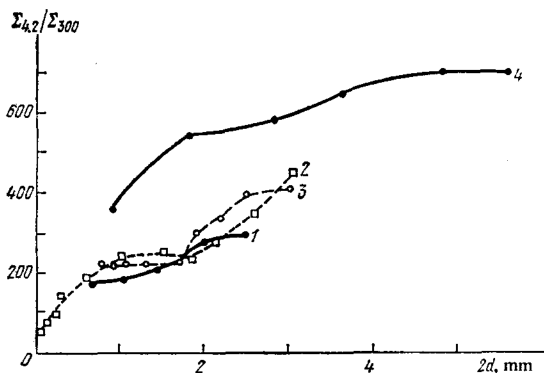


FIG. 13. Dependences of the electrical conductivity of Bi on its thickness at 4.2 °K: 1) from[66]; 2) from[72]; 3) from[75]; 4) from[80].

$d \ll l_p$; this may be attributed to the specular component of the scattering.[73,74]

These observations are in agreement with the interpretation based on anisotropic size effects. However, there are also some difficulties. The fall of $\Sigma$ by a factor of six in Fig. 12 can be explained only if the contribution of holes to the conductivity is $\lesssim 10\%$; however, according to[69], the contribution is $\approx 25\%$. The theory (Fig. 11) cannot account for a fall as steep as that exhibited by curve 3 in Fig. 13; however, since other curves (particularly, curve 4) are much smoother, we cannot exclude a possible influence of inhomogeneities, particularly in wedge-shaped samples. The greatest difficulty arises from the large anisotropic size effect observed for the orientation along which it can appear only as a result of a small inclination (≈6°) electron ellipsoids relative to the basal plane (curve 2); the cause of this is not clear.

In this connection, we must mention other attempts to explain the size effect. It is hypothesized in[75] that the effect is due to the drag of phonons and their scattering by the surface; subsequent extimates[76] and the results reported in[77] indicate that these should be weak effects. The saturation of $\Sigma$ in the range of small values of $d$ is explained in[59] by the specular scattering of glancing electrons but this mechanism may be active only in the range $d \lesssim l_p$.

Clearly, a more direct manifestation of the anisotropic size effect is the appearance of a dimensional transverse field $E_y$. The first report of such a field with $(\bar{E}_y/E_x)_{max} \approx 20$ was made in[78]. More detailed investigations were described in[79,80] (Fig. 14). The values of $\bar{E}_y/E_x$ at high temperatures, when the size effect disappeared, governed the constant contribution associated with the anisotropy of the bulk conductivity and a possible relative shift of the measuring electrodes. An estimate

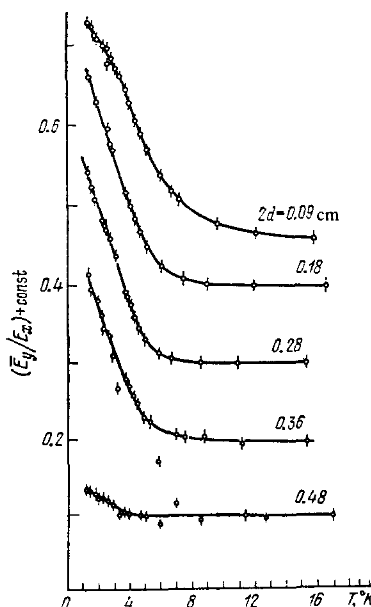


FIG. 14. Temperature dependences of the average transverse field $\bar{E}_y$ in samples of different thicknesses.[79]

based on the diffusion theory formulas, similar to Eq. (2.4), demonstrated that, in the case of Bi, the maximum value of this ratio was $(\bar{E}_y/E_x)_{max} \approx 0.5$; the results reported in[79,80] were in agreement with this value. It was assumed in[79,80] that the onset of the rapid fall of the curves in Fig. 14 corresponded to $L(T) \sim d$ and this was used in the determination of the temperature dependence $\tau_v(T)$ which agreed with the dependence $\tau_r(T)$ deduced from the acoustomagnetoelectric effect.[5]

The first experimental studies of the size-effect-related transverse magnetoresistance of Bi were carried out at 77 °K and interpreted as the "diffusion size effect."[18] However, according to[5], Bi is characterized by $\tau_p < \tau_v$ only at temperatures $T < 15$ °K; therefore, the anisotropic size effect should only be manifested at low temperatures. The measurements of the transverse magnetoresistance were carried out in[66] at 4.2 °K for samples with $d > L_v(H)$ in fields $H$ up to 2 kOe. The measured dependence of the size-effect component of $\Sigma$ on $H$ agreed with the theory in fields $H \sim 100$ Oe; deviations at higher values of $H$ were attributed to the dependence $s_v(H)$. The measured values of $\tau_v$ exhibited a large scatter and were an order of magnitude lower than those reported in[5]. Velocities of $s \sim 10^6$ cm/sec, deduced for various orientations of $H$, did not agree in the limit $H \to 0$ even for a single face. Thus, the reliability of the results obtained was problematic. Purer samples and stronger fields $H$ (Fig. 15) were used in[81]. Estimates of the parameters obtained in[81] gave $\tau_v \approx 2 \times 10^{-8}$ sec, in accordance with[5]. The surface recombination probability, estimated on the basis of a model with a single-valley electron and hole spectrum,[67] was $w_{np} \sim 1/3$. This value of $w_{np}$ corresponded to the range $s_r \gg L_r/a\tau_r$, and, therefore, the observed size effect clearly corresponded to a characteristic length $D/s_r$ (Sec. 2F). Studies of the size effect in Sb were reported in[82,83].

It is worth noting that there are no grounds for expecting semimetals to exhibit significant effects associated with energy relaxation (Sec. 2B). In fact, in the range $T \ll \varepsilon_F$, the change in $a_\alpha(\varepsilon)$ (Sec. 2C) is small at energies $\sim T$. Moreover, in the case of Bi, $c_s p_F$ is of the order of a few degrees and, therefore, at $T = 4$ °K, we have $\tau \sim \tau_p$. Some complications may arise only when the phonon mechanism begins to dominate the intervalley scattering ($T \gtrsim 6$ °K in the case of Bi[5]) so that the intervalley redistribution produces a secondary flux of hot electrons of energy $\omega_{ph} \approx 40$ °K[5] from one valley to another (Sec. 2C).

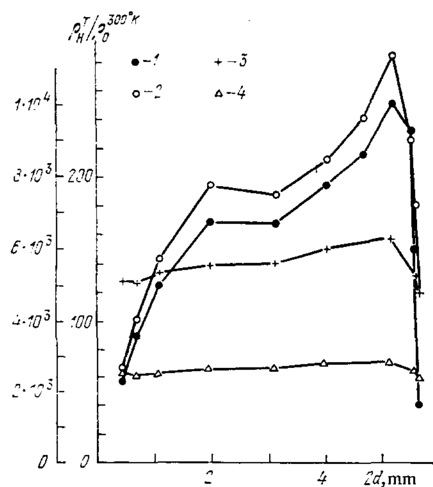


FIG. 15. Dependences of the magnetoresistance on the thickness $2d$ of a sample of rectangular cross section[81] in $H \parallel C_3$. The abrupt drop in $\rho(H)$ on the extreme right is due to the removal of a damaged surface layer. 1) $T = 4.2$ °K, $H = 1$ kOe; 2) $T = 4.2$ °K, $H = 10$ kOe (left-hand scale); 3) $T = 14$ °K, $H = 5$ kOe; 4) $T = 20$ °K, $H = 5$ kOe.

It is worth noting the following circumstance. The diffusion lengths $L$, associated with the intervalley scattering and recombination, are very large (of the order of millimeters) in Bi and, therefore, the preparation of samples $L$ presents no difficulties. In spite of that, there is a considerable scatter of the experimental results obtained by different workers. This may largely be due to the absence of any standard procedure for surface treatment and monitoring of the surface state. It is known that the surface treatment has a strong influence on the transport coefficients[68,81,155]: this influence is clearly due to a change in the conditions of motion of carriers in the surface layer because of the influence of etching on the magnitude and sign of the surface potential $\varphi_s$ (Sec. 2F). Interesting possibilities of direct experimental determination of the influence of the surface treatment on the specularity coefficient are provided by studies of the focusing of carriers in a transverse magnetic field.[156] Another possible cause of the scatter of the experimental results is clearly insufficient control of the bulk parameters of bismuth and of the degree of spatial homogeneity of these parameters. The high plasticity of Bi makes it difficult to avoid the generation of large numbers of dislocations: since it is natural to expect strong intervalley scattering of carriers by dislocation cores, plastic deformation can have a considerable influence on the size effect. This influence on the transport coefficients of bismuth is reported in[157].

## 3. ELECTRICAL PINCH EFFECT IN AMBIPOLAR SEMICONDUCTORS

In this section, we shall consider the behavior of an anisotropic ambipolar semiconductor in a strong electric field. An anisotropic ambipolar drift concentrates carriers from a large part of a sample in narrow layers, where the carrier density becomes much higher than the equilibrium value; we shall call these the pinch layers. Thus, a sample as a whole may be strongly depleted of carriers or may exhibit a strong carrier accumulation. The large diffusion lengths ($L_r \sim 0.1$–$1$ mm) mean that, at room temperature, high fields begin from $E_L \sim 1$ V/cm and complications associated with heating (Sec. 4) are unimportant. Large values of $L_r$ make it possible to observe the pinch effect in "ordinary" samples, i.e., the effect is not confined to thin layers. Consequently, the various aspects of this effect have been investigated in numerous experiments performed on anisotropic samples as well as on isotropic samples in a magnetic field. The theory has been compared in

detail with the experimental results.

### A. Physical situation and theory

We shall consider a plate made of an intrinsic semiconductor whose electron and hole mobility tensors ($u^n_{ij}$ and $u^p_{ij}$) are nondiagonal when expressed in terms of the axes linked to the plate. Using Eqs. (1.5), (1.11), and (1.12) and the quasineutrality condition (1.6), we obtain the following equation for the transverse ambipolar diffusion

$$\frac{d^2p}{d\eta^2} + 2\gamma \frac{dp}{d\eta} = p - p_i, \quad \gamma = \frac{aeL}{4T} = \frac{a}{4}\frac{E_x}{E_L}, \tag{3.1}$$

subject to the boundary conditions $\eta = \pm\,\delta$:

$$\left(\frac{dp}{d\eta}\right)^{\pm} + 2\gamma p^{\pm} = \mp S^{\pm}(p^{\pm} - p_i); \tag{3.2}$$

here, $a = a_n - a_p$ is analogous to Eq. (2.1); $L = L_r = \sqrt{D\tau_r}$; $D$ is the ambipolar diffusion coefficient defined by $D = 2D^n_{yy} D^p_{yy}/(D^n_{yy} + D^p_{yy})$; $\eta = y/L$; $\delta = d/L$; $S = sL/D$; $p_i$ is the equilibrium hole density. The coefficient $2\gamma$, which occurs in Eq. (3.1) in front of the first derivative, is the dimensionless effective transverse field which ensures the ambipolar drift in the $y$ direction.

The solution of Eq. (3.1) gives two characteristic lengths:

$$L_{1,2} = \frac{L}{\sqrt{1+\gamma^2} \mp \gamma}. \tag{3.3}$$

In high fields $\gamma^2 \gg 1$, which will be of prime interest to us later, we find that

$$L_1 \to L(E) = 2|\gamma| L = \frac{u}{2}|aE_x|\tau, \quad u = \frac{eD}{T}, \tag{3.4}$$

i.e., this length becomes the drift (extended diffusion) length, and

$$L_2 \to l(E) = \frac{L}{2|\gamma|} = \frac{2T}{|aeE_x|} \tag{3.5}$$

becomes the contraction diffusion length.[84]

If $aE_x > 0$, the effective field drives the carriers toward the $\eta = -\,\delta$ surface. Consequently, a depletion layer of thickness $\sim L(E)$ extends from the $\eta = \delta$ surface into the sample, whereas an accumulation pinch layer of thickness $\sim L(E)$ forms at the $\eta = -\,\delta$ surface. In the limit $2\gamma \gg \delta$, $\delta^{-1}$, $S^+$, $1/S^-$, the depletion region extends over almost the whole crystal and, in this region, the hole density is $p \approx p_i(S^+ + \delta - \eta)/2\gamma$, i.e., the density decreases proportionally to $E_x^{-1}$. In the pinch layer, the maximum density reaches saturation: $p^- \approx p_i(S^+ + S^- + 2\delta)/S^-$, and the total number of carriers decreases proportionally to $E_x^{-1}$. Consequently, the current through the sample becomes saturated. Its value depends on $S^{\pm}$ and rectification is observed for $S^+ \neq S^-$.

There are several special situations which are exceptions to the above rules. If $S^+ = \infty$, the carrier density throughout almost the whole of the crystal is $\approx p_i$ and, in the pinch layer, the carrier density increases proportionally to $\gamma$ near $\eta = -\,\delta$; as a result, we have $i_x \propto \gamma$. If $S^- = 0$, we find that the density obeys $p^- \propto \gamma$ and the current is $i_x \propto \gamma$. If we have both $S^+ = \infty$ and $S^- = 0$, then $p^-$ and $i_x$ are both proportional to $\gamma^2$. In the latter case, the rectification effect is strongest: the reverse current saturation is minimal and the forward current rises proportionally to $E_x^2$.

These results apply equally well to an isotropic semiconductor in a magnetic field and to an arbitrary anisotropic semiconductor. In the latter case, the redistribution of carriers is known as the electrical pinch effect; we shall adopt this term for all the related phenomena. The formal difference is that, in the case of a magnetic field, the tensors $u^{\alpha}_{ij}$ have an antisymmetric part.

We must stress in conclusion that, in contrast to Sec. 2a, the effects discussed here are mainly due to a change in the carrier density and are governed by the parameter $\gamma$, whereas changes in the conductivities of the order of $a^2$ (corresponding to the substitution $\sigma \to \sigma^*$, as shown in Sec. 1B) play a secondary role.

### B. Electrical pinch in homogeneous samples—experimental results

Direct observations of the redistribution of carriers under the electrical pinch conditions were made in[85] using the absorption of light by free carriers. The measurements were carried out on intrinsic Ge subjected to a uniaxial stress. The experimental dependences (Fig. 16) yielded directly the distributions of carriers in a sample for small values of $s^{\pm}$ (Fig. 16a) and for small $s^-$ but large $s^+$ (Fig. 16b). Depletion regions extended over a large part of the sample, pinch layers were observed (where the carrier density increased by an order of magnitude), and both depletion and accumulation of the carriers in the sample as a whole were found, depending on the direction of the current (Fig. 16b). It should be stressed that all the curves were obtained for small values of $a$ ($\approx$0.7 to 0.1) and the nonlinearity appeared in weak fields because of the smallness of $E_L$(~0.1 V/cm). A change in the carrier density near the surface was also deduced from the reverse current across a local $p$-$i$ junction[86] (Fig. 17).

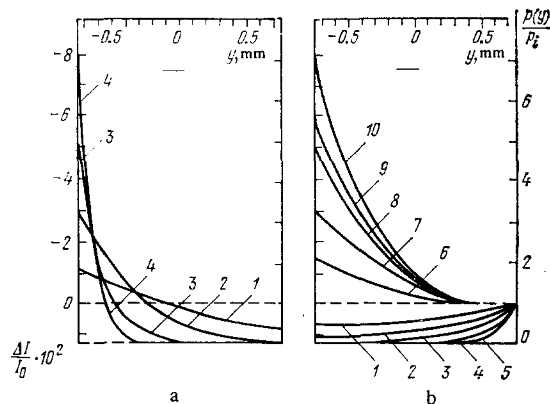


FIG. 16. Changes in the transmission of infrared radiation (left-hand scale) and transverse distribution of the carrier density (right-hand scale)[118] for a sample with $2d = 1.5$ mm, $L = 2$ mm, $T = 50\,^{\circ}$C; deforming stress $X = 1500$ kg/cm$^2$; $E \equiv E_x$: a) $s^- \approx s^+ \approx 10^2$ cm/sec, $E$ (V/cm) = 20, 40, 60, and 100 (curves 1–4 respectively); b) $s^- \approx 10^2$ cm/sec, $s^+ \approx 10^4$ cm/sec, $E$ (V/cm) = −5, −10, −15, −20, −30, 5, 10, 15, 20, and 30 (curves 1–10, respectively). The horizontal segments in the upper part of the figure denote the size of an infrared illumination spot.

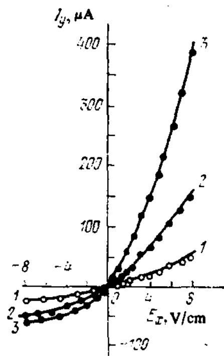

FIG. 17. Dependences of the current $I_y$ through a $p$–$i$ junction on the external field $E_x$, plotted for different pressures $X$ producing uniaxial deformation ($s^- \ll s^+$).[86] The $p$–$i$ junction was formed by local alloying a side $(x, z)$ surface ($y = -d$) of an intrinsic Ge crystal with indium. An ohmic contact was formed on the opposite surface. Pressure $X$ (kg/cm$^2$) = 400, 800, and 1200 (curves 1–3, respectively).

The current-voltage characteristics of a plate were of the type shown in Fig. 18. All the features predicted above were observed: strong nonlinearity and rectification, saturation of the current (the residual slope was due to the fact that $n_0 - p_0 \neq 0$), and even superlinearity of the forward current $i_x \propto E_x^2$ in moderate fields.

The main feature of the carrier kinetics was the dominant role of the ambipolar transverse drift. Therefore, when carriers were driven to the surface characterized by a large value of $s$, the relaxation time was identical with the drift time $2d/|(a/2)uE_x| \propto E_x^{-1}$. The kinetics was also investigated in[87–89].

The effects described in Sec. 3A should be observed not only for equilibrium carriers but also in the case of photoexcitation of electron–hole pairs. The photocurrent characteristics (Fig. 19) were reported to exhibit a strong saturation[87,90]; the origin of this saturation was the same as in an intrinsic semiconductor.

The electrical pinch effect was observed not only in deformed Ge but also in two naturally anisotropic semiconductors: CdSb[91] and Te.[92]

It was suggested in[85] that the qualitative changes in the asymptotes of the current-voltage characteristics under uniaxial deformation could be used in the construction of highly sensitive strain gauges.

### C. Electrical pinch in magnetic fields

The theory of the electrical pinch effect in magnetic fields was started in[8] and developed in several papers.[10,12,93–96,etc.] The very first experimental investigations revealed rectification of the current in the case of strong asymmetry of $s^+$ and $s^-$ (in this connection, the concept of a magnetic blocking layer was introduced[9,11]), nonlinear current-voltage characteristics with a tendency to saturation of the type shown in Fig. 18, influence of light on magnetic blocking layers, reduction in the relaxation times with increasing $E_x$ and $H_z$, luminescence due to nonequilibrium carriers,[97] and so on. An advantage of measurements in a magnetic field is the practically unlimited range of variation of the

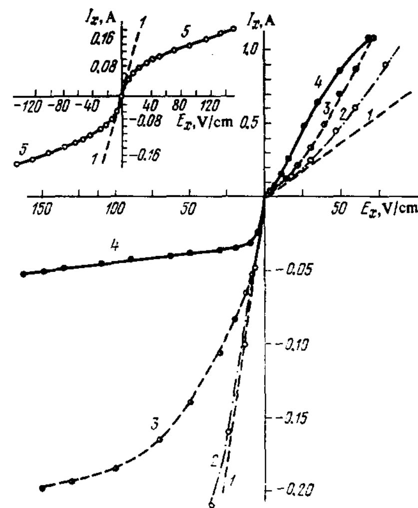

FIG. 18. Current-voltage characteristics of the same samples as in Fig. 16[85]: 1) undeformed sample ($X = 0$); 2)–4) rectifying characteristics of a sample with $s^- \approx 10^2$ cm/sec, $s^+ \approx 10^4$ cm/sec, subjected to pressures $X = 100$, 300, 1500 kg/cm$^2$ (curves 2–4, respectively); 5) nonrectifying characteristics of a sample with $s^+ \approx s^- \approx 100$ cm/sec, subjected to $X = 1500$ kg/cm$^2$.

anisotropy parameter $a$, whereas, in an anisotropic situation in $H = 0$, we always have $a < 1$ and the range of its variation as a result of deformation is even less. The phenomena occurring in magnetic fields can be used in measuring the parameters of semiconductors such as $s^\pm$, $\tau$, and $D$, and in the determination of the magnetic field itself. We shall not consider these points in greater detail because a review of the earlier work can be found in Beer's monograph[98]; the number of papers published on this subject is now about 100.

### D. Electrical pinch in bent samples[99]

An ingenious variant of the electrical pinch effect is reported in[99]. If uniaxial compression (Sec. 3B) is replaced with bending, the deformation in a plate and, consequently, the anisotropy parameter $a(y)$ become linear functions of $y$:

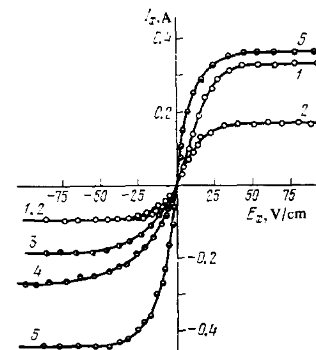

FIG. 19. Photocurrent-voltage characteristics of intrinsic Ge at room temperature ($2d = 0.15$ cm, $L = 0.21$ cm).[87] The $y = -d$ surface was illuminated with strongly absorbed light ($3 \times 10^{17}$ photons/cm$^2$): 1), 2) $s^+ \to \infty$, $X = 1200$ kg/cm$^2$, $s^-(1) < s^-(2)$; 3), 4) $s^+ \to \infty$, $s^-(3) = s^-(4) = s^-(1)$, $X(3) = 600$ kg/cm$^2$, $X(4) = 400$ kg/cm$^2$; 5) $s^+ \approx s^-$, $X = 1200$ kg/cm$^2$. Only the reverse branches are shown for curves 3 and 4.

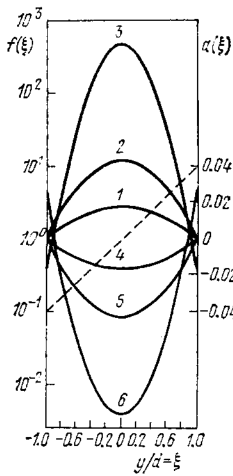


FIG. 20. Transverse distribution of the dimensionless carrier density $f = p(y)/p_i$ in a sample with $\delta=0.125$, $a_0 = 0.04$, plotted for different values of the dimensionless electric field $\gamma_i = a_0 edE_x/2T$ in the case of "forward" (1–3) and "reverse" (4–6) bending.[99] The dashed line gives the dependence $a(y)$. 1), 4) $\gamma_1 = \pm 2$; 2), 5) $\gamma_1 = \pm 5$; 3), 6) $\gamma_1 = \pm 15$.

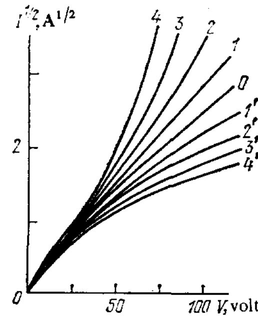


FIG. 22. Experimental current-voltage characteristics, $I^{1/2} = f(V)$, of a bent germanium diode (dimensions $2d=1.1$ mm, $l_z = 3.5$ mm, $l_x = 5.5$ mm, [104] plotted for different pressures $X_0$: 0) 0; 1), 1') 100; 2), 2') 200; 3), 3') 300; 4), 4') 400 kg/cm$^2$. The unprimed numbers correspond to forward bending and the primed numbers to reverse bending.

$$a(y) = a_0 y/d. \qquad (3.6)$$

A bent plate is compressed on one side of the neutral plane and stretched on the other. Therefore, the directions of the transverse drift are opposite on the two sides of the neutral plane. Consequently, if $s^+ = s^-$, a density extremum is established in the neutral plane: it can be a maximum or a minimum, depending on the direction of the current. Calculated distributions are plotted on a logarithmic scale in Fig. 20.

The current-voltage characteristics corresponding to $s^+ = s^-$ exhibit strong rectification: the forward direction corresponds to the presence of a pinch layer near the neutral plane and the reverse direction to the drift of the carriers from the bulk of the sample to two identical pinch layers at the surfaces, where the carriers rapidly recombine. The experimental current-voltage characteristics are in good qualitative agreement with the theory (Fig. 21).

### E. Related effects

1) *Electrical pinch in heating fields*. The electrical conductivity of a cubic crystal becomes anisotropic in

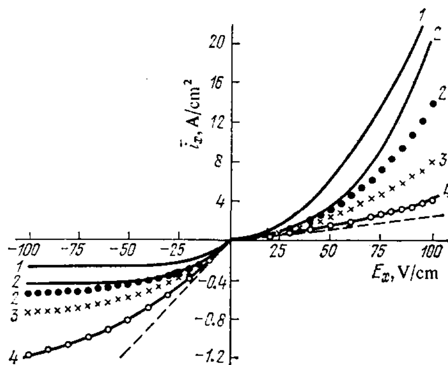


FIG. 21. Theoretical (curves) and experimental (points) current-voltage characteristics of bent samples of intrinsic Ge[99] plotted for $a_0 = 0.04$ (corresponding to $X_0 = 600$ kg/cm$^2$ applied to the surfaces $y = \pm d$): 1) $\delta = 1.0$; 2) $\delta = 45$; 3) $\delta = 0.312$; 4) $\delta = 0.125$. The dashed line represents the current-voltage characteristic of an undeformed sample ($X_0 = 0$).

heating fields (Sasaki effect).[31] It is pointed out in[14] that this anisotropy may itself be a cause of the electrical pinch effect. Such an effect was observed experimentally[100] in Ge subjected to fields of ~1 kV/cm and it was manifested by a strong dependence of the resistance on the orientation of a sample. The theory of this effect is presented in[101,102].

2) *Piezodiode effect*.[103,104] The electrical pinch effect also appears as a result of the injection of nonequilibrium carriers across a *p-n* junction. The special feature of this case is a strong inhomogeneity of the carrier distribution in the direction of the current (i.e., along the $x$ axis). A drift distribution of a nonequilibrium plasma is established when a strong field $E_x$ is applied to an isotropic long diode: the density varies in accordance with the law $p(x) \propto \sqrt{i_x \tau_{eff}/x}$ and the current-voltage characteristic is $i_x \propto \tau_{eff} V^2$, as shown in [105] (and then in[106]) and[107]. Here, $\tau_{eff}$ allows for the influence of surface recombination. By way of example, we shall consider the bending deformation. Under "reverse" bending when the plasma approaches the walls, we have $\tau_{eff} \sim l(E)/s \propto E_x^{-1}$, the current falls, and the current-voltage characteristic becomes ohmic. In the case of "forward bending," the injected plasma becomes detached from the walls, the recombination rate falls ($\tau_{eff} \to \tau_r$), the current rises, and the current-voltage characteristic of long samples retains the form $i \propto V^2$, whereas, in the case of shorter samples, injection breakdown is observed[108]: the voltage across the sample tends to saturation. All these features are demonstrated by the curves in Fig. 22, recorded for a plate-like germanium diode.

The current-voltage characteristics of samples subjected to homogeneous deformation are similar to those obtained under "reverse bending." The same characteristics are obtained in the magnetodiode effect[13] in

[13]The universal mechanism of the magnetodiode effect, based on the dependence of $L$ on $H$ due to the ordinary magnetoresistance, is suggested and investigated in[109–111]. This effect is weak in the plates under discussion here but it predominates in samples of different geometry.

thin plates.[103,112–114] Ambipolar transport in a different geometry is analyzed in[115].

3) *Electrical pinch in semiconductors with deep centers.* It is shown in[116] that the electrical pinch effect may occur in a semiconductor with an almost unipolar conduction (equilibrium densities $n_0 > p_0$) and a high trap concentration. The effect is then due to a strong asymmetry of the recombination times of electrons and holes, $\tau_p/\tau_n \ll 1$, and it is manifested by an almost complete capture of electrons by levels when holes are driven to the surface.

The results of the present section can be summarized as follows. The large value of the recombination length $L_r$ makes the electrical pinch experiments absolutely reliable and a wide range of phenomena can be studied. The agreement between the theory and experiment is complete and only special situations and technical applications need to be studied in future.

## 4. MANY-VALLEY CRYSTAL IN STRONG FIELDS

We shall now consider a very special nonlinear behavior in strong electric fields, which is exhibited by many-valley crystals. We shall show that electrons belonging to different valleys should become completely separated in space, filling separate layers (domains). In ambipolar situations, the holes should participate in this redistribution and this may result in giant changes in the conductivity.

### A. Unipolar conduction. Domains[117,118]

We shall assume that the field $E_x$ is sufficiently strong. The intervalley redistribution is then considerable either throughout the sample or at least in its surface parts. The transverse component of the $\alpha$-electron current is

$$j_{\alpha y} = -u_{\alpha yy} n E_x \left[ \left( a_\alpha + \frac{E_y(y)}{E_x} \right) f_\alpha + \frac{T}{E_x} \frac{df_\alpha}{dy} \right] \quad (\alpha = 1, 2, \ldots, \nu), \tag{4.1}$$

where $\nu$ is the number of valleys, $f_\alpha(y) = n_\alpha(y)/n$, $n$ is the equilibrium electron density, so that the neutrality condition is $\sum_{\alpha=1}^{\nu} f_\alpha = 1$. Although Eq. (4.1) applies to nondegenerate electrons, the basic conclusions are valid more generally.

We shall first consider a plate of thickness $2d$. Then, provided the bulk and surface intervalley scattering rates are finite, the currents $j_{\alpha y}$ remain finite when the field $E_x$ is increased. Therefore, in high fields $E_x$, we have

$$\left( a_\alpha + \frac{E_y}{E_x} \right) f_\alpha + \frac{T}{E_x} \frac{df_\alpha}{dy} = O\left( \frac{E_L}{E_x} \right). \tag{4.2}$$

Since $f_\alpha \leq 1$, the term with the derivative may play an important role only in layers whose thickness is of the order of the contracted length $l(E) \sim T/aeE_x$. Inside such layers, we have

$$\left( a_\alpha + \frac{E_y}{E_x} \right) f_\alpha = O\left( \frac{E_L}{E_x} \right) \quad (\alpha = 1, 2, \ldots, \nu). \tag{4.2'}$$

The solutions of the system (4.2′), satisfying the neutrality condition in the limit $E_x \to \infty$, are

$$f_\beta(y) = \delta_{\beta\alpha}, \quad E_y = -a_\alpha E_x \quad (\alpha, \beta = 1, 2, \ldots, \nu). \tag{4.3}$$

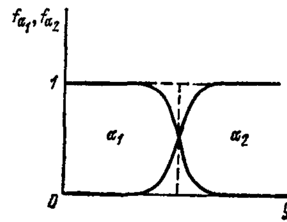

FIG. 23. Distributions of $\alpha_1$ and $\alpha_2$ electrons in a domain ($\alpha_1$-$\alpha_2$) wall.

Consequently, electrons form domains, which are layers parallel to the surfaces of the plate. Each domain contains electrons of one type and, in the case of the $\alpha$-electron domain (briefly, $\alpha$ domain), we have $E_y = -a_\alpha E_x$.

It remains to determine the law governing the relative positions (sequence) of the domains and to calculate their thickness.

We shall consider a hypothetical wall between $\alpha_1$ and $\alpha_2$ domains (Fig. 23). In this wall, we have $f_{\alpha_1} + f_{\alpha_2} = 1$, where $f_{\alpha_1}$ falls from 1 to 0, $f_{\alpha_2}$ rises from 0 to 1, and $E_y/E_x$ varies from $-a_{\alpha_1}$ to $-a_{\alpha_2}$. It follows from Eq. (4.2) that

$$\frac{d}{dy} \ln \frac{f_{\alpha_1}}{f_{\alpha_2}} = -\frac{E_x}{T} (a_{\alpha_1} - a_{\alpha_2}), \tag{4.4}$$

and, therefore, if $E_x > 0$, such a wall can only exist if $a_{\alpha_1} > a_{\alpha_2}$, i.e., if domains are distributed along the $y$ axis in monotonically decreasing order of $a_\alpha$. If $E_x < 0$, they are distributed in increasing order of $a_\alpha$.

The thickness of $\alpha$ domains, $d_\alpha$, is governed by the overall balance of intervalley transitions in a sample. If there is no surface intervalley scattering, a redistribution of $\alpha$ electrons in a sample does not alter their total number and $\delta_\alpha = d_\alpha/2d = f_\alpha^0$, where $f_\alpha^0$ are the equilibrium values of $f_\alpha$. In the case of equivalent valleys, we have $f_\alpha = 1/\nu$ and all the thicknesses $d_\alpha$ are the same. In the "degenerate" case of $a_{\alpha_1} = a_{\alpha_2}$, a domain of twice the normal thickness is filled uniformly with $\alpha_1$ and $\alpha_2$ electrons. However, if $s_{\alpha\beta}^{\pm} \neq 0$, the number of layers $\nu'$ does not always agree with the number of domains: $\nu' \leq \nu$, or the outer domains may be expelled from a sample completely and their electrons confined to surface walls $\sim l(E)$ thick (Fig. 24). A system of equations which describes an overall balance for each of the $\nu$ groups of electrons

$$\sum_{\substack{\beta=1 \\ \beta\neq\alpha}}^{\nu} (\tau_{\alpha\beta}^{-1}\delta_\alpha - \tau_{\beta\alpha}^{-1}\delta_\beta + \mathscr{S}_{\alpha\beta}^{+} f_\alpha^{+} - \mathscr{S}_{\beta\alpha}^{+} f_\beta^{+} + \mathscr{S}_{\alpha\beta}^{-} f_\alpha^{-} - \mathscr{S}_{\beta\alpha}^{-} f_\beta^{-}) = 0 \quad (\alpha = 1, 2, \ldots, \nu) \tag{4.5}$$

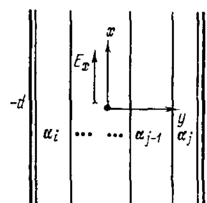

FIG. 24. Distribution of domains in a plate ($a_{\alpha_i} < a_{\alpha_j}$): electrons with $a_{\alpha_s} < a_{\alpha_i}$ are concentrated near the $y = -d$ surface and those with $a_{\alpha_s} > a_{\alpha_j}$ are concentrated near $y = d$.

consists of $(\nu - 1)$ independent equations; here $^{\pm}_{\alpha\beta} = s^{\pm}_{\alpha\beta}/2d$, $f^{\pm}_{\alpha} = f_{\alpha}(\pm d)$. This system and the conditions

$$\sum_{\alpha=1}^{\nu} \delta_\alpha = \sum_{\alpha=1}^{\nu} f_\alpha^{+} = \sum_{\alpha=1}^{\nu} f_\alpha^{-} = 1, \qquad \delta_\alpha f_\alpha^{\pm} \geqslant 0 \tag{4.6}$$

yield $\nu'$ nonzero thicknesses $\delta_\alpha$ and $\nu - \nu' = 2$ nonzero values of $f^{\pm}_{\alpha}$ corresponding to electrons in the two outer domains and $\nu - \nu'$ expelled domains.

For example, in the case of a two-valley semiconductor $(a_1 < a_2)$ with $\mathscr{S}^{+} \neq \mathscr{S}^{-}$, there are two domains with $\delta_{1,2} = (1/2)[1 \pm (\mathscr{S}^{-} - \mathscr{S}^{+})\tau]$, as long as $\tau\,|\mathscr{S}^{-} - \mathscr{S}^{+}| < 1$, and $\delta_1 = 1$, $\delta_2 = 0$, $f_2^{-} = (\mathscr{S}^{+} + \tau^{-1})/\mathscr{S}^{-}$, $f_1^{-} = (\mathscr{S}^{-} - \mathscr{S}^{+} + \tau^{-1})/\mathscr{S}^{-}$ if $\tau(\mathscr{S}^{-} - \mathscr{S}^{+}) > 1$, i.e., the first domain expands so as to fill the whole sample with the exception of a thin layer near the $y = -d$ surface.

Inside a domain, the density varies over the intervalley drift length $L(E) \sim a u E_x \tau$ and, in the walls, it varies over the length $l(E)$. Therefore, the criteria for the appearance of the pattern described above are

$$\text{a) } l(E) \ll d \ll L(E), \qquad \text{b) } S \ll \frac{L(E)}{L}. \tag{4.7}$$

The first of them may be satisfied only by thin plates for

$$\left(\frac{aE_x}{E_L}\right)^2 \gg 1, \tag{4.7'}$$

which is the reverse of the criterion (2.6).

The criterion "a" of Eq. (4.7) cannot be satisfied in thick samples. In such samples, a strong intervalley redistribution occurs at distances $\lesssim L(E)$ from the surfaces. The structure formed consists of layers of thickness $\sim L(E)$ in which there are several types of electrons whose densities vary smoothly; the layers are separated by walls $\sim l(E)$ thick. An example of this distribution is shown in Fig. 25.

## B. Transport coefficients of sample with domain structure

We shall now consider some experimental manifestations of the domain structure. The effective electrical conductivity in a high field is[117]

$$\Sigma_\infty(d) = n \sum_{\alpha=1}^{\nu} u_\alpha^* \delta_\alpha, \quad u_\alpha^* = u_{xx}^\alpha - \frac{u_{xy}^\alpha u_{yx}^\alpha}{u_{yy}^\alpha}. \tag{4.8}$$

The subscript in $\Sigma_\infty$ shows that we are considering the value in the limit $E_x \to \infty$; the mobilities $u^*_\alpha$ are one-dimensional analogs of the conductivities in Eq. (1.9). If $s^{\pm}_{\alpha\beta} = 0$, we have $\delta_\alpha = f^0_\alpha$ in all cases and $\Sigma_\infty(d)$ is equal to $\Sigma_0(0)$, which is the conductivity in a very thin plate

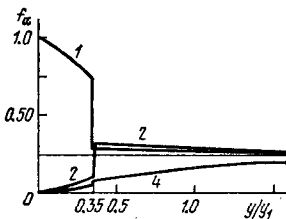


FIG. 25. Distributions of relative densities of $\alpha$ electrons. $f_\alpha(y)$, near the (010) surface of a semi-infinite $(y > 0)$ sample of $n$-type Ge.[117] The current is assumed to flow along the [101] axis; $a_1 = -a_4$, $a_2 = a_3 = 0$; 1) $f_1(y)$; 2) $f_2(y) = f_3(y)$; 4) $f_4(y)$; $y_1 = (u_t - u_l)E_x\tau/6\sqrt{2}$

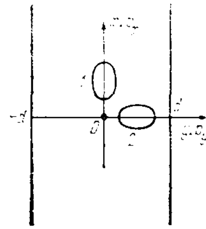

FIG. 26. Two-valley semiconductor which has no domain structure $(a_1 = a_2 = 0)$ in $H_z = 0$. The magnetic field $H_z$ results in $a_1 \neq a_2$ and in the appearance of a domain structure.

in a weak field given by Eq. (1.9); the subscript in $\Sigma_0$ indicates that we are considering the limit $E_x \to 0$. Therefore, $\Sigma_\infty(d) = \Sigma_0(0) \leqslant \Sigma_0(d)$ (Sec. 2a). If $s^{\pm}_{\alpha\beta} \neq 0$, we also have cases with $\Sigma_\infty(d) > \Sigma_0(d)$, and the differences between these two conductivities may be considerable. The letter index of $\Sigma$ is the ratio $u_l/u_t$ of the principal mobilities in one ellipsoid. For cubic crystals and $d < L_v$, the conductivity is $\Sigma_0(d) \approx \sigma$, and the minimum and maximum values of the ratio $\Sigma_\infty(d)/\sigma$ for $u_l \ll u_t$ are $3u_l/2u_t$ and $3/2$. If $s^{+} \neq s^{-}$, the conductivity $\Sigma_\infty$ depends on the sign of $E_x$ (rectification effect).

The magnetoresistance of a domain structure is due to the influence of the field $H_z$ on $a_\alpha$. Therefore, $H_z$ may alter the domain sequence; if the domains which interchange places correspond to different values of $\delta_\alpha$, the conductivity $\Sigma_\infty$ changes abruptly. The simplest example is a two-valley semiconductor with the geometry shown in Fig. 26. If $H_z = 0$, we find that $u_{1yx} = u_{2yx} = 0$ and we have just one uniformly filled 1-2 domain. If $H_z \neq 0$ and $s^{+} \neq s^{-}$, there are two domains of different thickness. If $\tau\,|\mathscr{S}^{-} - \mathscr{S}^{+}| > 1$, one domain fills the whole sample and the second is expelled. Depending only on the sign of $H_z$, either domain 1 or domain 2 is retained; consequently, we have either $\Sigma_\infty \approx n u_{1xx}$ or $\Sigma_\infty \approx n u_{2xx} \approx n u_{1yy}$, and, at the point $H_z = 0$, the conductivity $\Sigma_\infty$ changes abruptly by a factor $u_t/u_l$.

Even if $H_z = 0$, a quasi-Hall emf is established[117] and its order of magnitude is $aE_x \min\{d, |s^{-} - s^{+}|\tau\}$. The conductivity in the case of a weak transverse current is limited by the intervalley scattering and is of the order of $\sigma/L(E)$, which is less than the equilibrium conductivity $\sigma/2d$ by a factor $\sim L(E)/d \gg 1$.

## C. Ambipolar conduction. Photoconductivity[35,119-121]

In unipolar crystals, the scale of the effects is limited by the fact that only the effective carrier mobility changes whereas the total number of carriers remains constant, and redistribution is significant only over distances which do not exceed the extended intervalley length. We shall show that, in an ambipolar system, the amplitude and spatial scales may increase considerably, the former because of a large change in the total number of carriers and the latter because of the activation of the electron–hole recombination and because of the length $L_r$.

Many-valley effects should be manifested at low temperatures when $\tau_v$ is large. Under these conditions ambipolar and intrinsic conduction exist only during illumination (photoconductivity), or in narrow-gap and zero-gap semimetals and semiconductors (see, for ex-

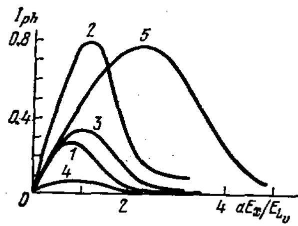


FIG. 27. Field dependences of the photocurrent in a semi-infinite ($y>0$) two-valley semiconductor ($a_1=-a_2=a$).[119] Here, $I_{ph}$ is the dimensionless photocurrent; $L_v/L_r=10^{-2}$; 1) $s_v=0$, $s_r=1$, 2) $s_v=0$, $s_r=0.1$; 3) $s_v=1$, $s_r=1$; 4) $s_v=1$, $s_r=10$; 5) $s_v=10$, $s_r=1$.

ample,[122]). We shall consider these two cases simultaneously.

We shall discuss the specific case of a hole with an isotropic spectrum and electrons with a many-valley spectrum. We then have two different situations: $n\gg p$ and $n\lesssim p$.

In the former case, the intervalley redistribution in high fields $E_x$ at the surface produces a strong field $E_y\sim aE_x$ directed toward the surface in a layer of thickness $\sim L_v(E)$. This new field creates a surface potential well for holes and the depth of this well is $\sim aE_xL_v(E)$, which ensures that the effective value of $s_r$ increases by the factor $\exp[(eaE_xL_v/T)^2]$. As a result, bulk excitation produces a depletion layer, $\sim L_r$ thick. In the case of surface excitation, a retarding field increases the rate of surface recombination so much that the photocurrent decreases exponentially in a certain range of $E_x$ (Fig. 27).

In the second case, we can conveniently describe the motion of carriers by the ambipolar diffusion coefficient

$$\left.\begin{aligned} D(E) &= D_pD_n\,[n+p(1+\gamma^2)]\,(nD_n+pD_p)^{-1},\\ \gamma^2 &= \frac{1}{\nu}\sum_{\alpha=1}^{\nu}(u^{\alpha}_{yx}E_x)^2\,\tau_vD_n^{-1}. \end{aligned}\right\} \qquad (4.9)$$

In the limit $\gamma\to 0$, this coefficient reduces to the ordinary coefficient and, beginning from $aE_x\gtrsim E_{L_v}$, it increases proportionally to $E_x^2$. The corresponding diffusion length $L_{rv}(E)=[D(E)\tau_r]^{1/2}$ increases proportionally to $|E_x|$. This increase is easily interpreted if we bear in mind that $\alpha$ electrons drift transversely under the action of a force $\sim eaE_x$, due to the field $E_x$. This force is random because of the intervalley scattering and, therefore, in a lifetime $\tau_r$, an electron diffuses in the $y$ direction to a distance $\sim auE_x\sqrt{\tau_v\tau_r}$, which agrees with the value $\sim L_{rv}(E)$ obtained above. Pinch layers of thickness $\sim l(E)$ are formed at both surfaces (as described in Sec. 3) and this increases the effective values of $s_r^{\pm}$. Consequently, depletion layers $\sim L_{rv}(E)$ thick are formed. Two types of current-voltage characteristic (Fig. 28) may be observed, depending on the ratio of the parameters. Samples with near-intrinsic conduction and with $s_v^{\pm}L_v<D$ and $s_r^{\pm}\tau_r>d$ exhibit $N$-type characteristics.

The second ohmic region in the characteristics corresponds to fields in which depletion layers spread over the whole sample and the majority carrier density is equal to the difference between the equilibrium densities $(n_0-p_0)$.

In all cases, the depletion is maximal for $n_0\approx p_0$, i.e., in an intrinsic semiconductor. If $n_0=p_0$, provided only $d\ll L_{rv}(E)$, the residual carrier density in the bulk is proportional to $1/E_x$. This density is high only in surface layers whose thickness is proportional to $1/E_x$, where it reaches a finite value in the limit $E_x\to\infty$. Therefore, the total number of carriers in a sample and, consequently, the conductivity decrease in proportion to $E_x^{-1}$ and the current tends to saturation. The exception is the case when the $x$ axis is parallel to the principal direction of one of the electron ellipsoids: the electrons in question and the same number of holes are then retained in the bulk and the conductivity remains finite.

It is interesting to note that the intervalley redistribution changes the photoconductivity even in the $s_v=\infty$ case. The number of photocarriers generated by strongly absorbed light is then not given by the usual formula $N=G\tau_r/(1+S_r)$ but by $N=G\tau_r$ which applies in strong fields $\gamma\gg 1$; here, $G$ is the rate of carrier generation.

Thus, in an ambipolar situation, the intervalley redistribution generates effects extending over distances $\sim L_r$ and even $\sim L_{rv}(E)$.

### D. Discussion of possibilities of observing postulated effects

The domain structures described in the present chapter and the associated nonlinear phenomena have not yet been investigated (to the authors' knowledge). Therefore, to facilitate the design of suitable experiments, we shall list here some of the experimental manifestations of the formation of such domains (layers) and we shall then discuss the conditions for the observation of these manifestations.

1) Sublinear current-voltage characteristics should be exhibited by unipolar samples: if $s^+\neq s^-$, rectification should be observed.

2) A transverse emf should appear in cubic crystals (for $s^+\neq s^-$).

3) Abrupt changes in the resistance and transverse emf should be observed when an external magnetic field alters the domain sequence. Kinks in the dependences of the same quantities on various parameters (deformation, values of $s^+$ and $s^-$, etc.) should occur when the

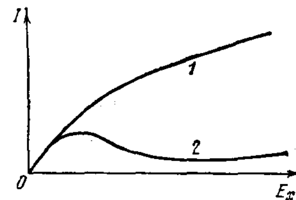


FIG. 28. Typical current-voltage characteristics of ambipolar many-valley semiconductors: 1) characteristic typical of non-intrinsic samples and of intrinsic samples with large values of $s_v$ and small values of $s_r$; 2) characteristic typical of intrinsic samples with small values of $s_v$ and large values of $s_r$.

number of domains in a sample changes.

4) There should be a special dependence of the photoconductivity on the field $E_x$ (Sec. 4c).

5) A strong anisotropy of the photoconductivity should be a feature of cubic crystals in very high fields.

The main difficulty is the heating of the electron gas. The average electron energy can be represented by $\varepsilon_\alpha = \varepsilon_0 + ev_\alpha E_x \tau_\varepsilon^\alpha$, where $v_\alpha(E_x)$ is the drift velocity. In the case of strong heating, the second term predominates and Eq. (4.7) changes to $v\tau_\varepsilon/a \ll d \ll av\tau_v$, which is possible only if $\tau_\varepsilon \ll a^2\tau_v$; this condition is essentially the same as the general criterion of the validity of the whole phenomenological theory of the present section. The second criterion of itself ensures the formation of a layer structure at the surface of a bulk semiconductor (end part of Sec. 4a). The first criterion applies to the domains in plates and is more stringent. A quantative agreement with the theory of Secs. 4a–4c requires that important parameters should not change as a result of heating. The strong temperature dependence $\tau_v \propto \exp(-\omega_{ph}/T)$ in the intervalley phonon scattering range requires in the replacement of (4.7′) with more stringent criteria:

$$\left(\frac{E_x}{E_{L\varepsilon}}\right)^2 \ll \frac{T}{\omega_{ph}}, \quad \tau_\varepsilon \ll \frac{a^2\tau_v T}{\omega_{ph}}.$$

The numerical values of $\tau_v$ and $\tau_\varepsilon$ of Ge have now been reliably estimated. If the donor concentration is $\approx 10^{12}$ cm$^{-3}$ at $T \approx 20$ °K, it follows from extrapolation of the results in[2] that $\tau_v \approx 2.5\times10^{-7}$ sec. The time $\tau_\varepsilon$, estimated for the acoustic scattering, is of the order of $5\times10^{-10}$ sec. This means that the second stringent criterion is satisfied well.

## 5. SKIN EFFECT IN SEMIMETALS

In semimetals, a skin layer, which is penetrated by an external electromagnetic field, acts as a "plate" where anisotropic size effects are observed. The intervalley redistribution results in the participation of carriers from various valleys in the oscillatory process. Consequently, mixed electromagnetic–density waves are are generated; their number increases and the depth of penetration changes considerably. The electron–phonon coupling means that the densities create deformations in the lattice, i.e., they generate sound; this conversion of electromagnetic into acoustic waves is a very effective mechanism.

### A. Influence of intervalley distribution on skin effect

We have assumed so far that the applied electric field is homogeneous and, therefore, a redistribution of carriers appears only where the spatial homogeneity of the system is disturbed: this happens—with the exception of the two cases considered in Sec. 3D and at the end of Sec. 2A—only near the surfaces of a sample. A completely different situation is established in an alternating field: the field inhomogeneity in a distance of one wavelength results (because of the anisotropy of the mobility tensors $u_{ij}^\alpha$) in inhomogeneous fluxes in the direction of wave propagation and, consequently, it produces nonequilibrium carriers. Since, in this case, nonequilibrium carriers are generated not only on the surface but also in the bulk, the effect does not disappear even if $s \to \infty$. Under the skin effect conditions, the pattern resembles that discussed in Sec. 2A in the case of a surface accumulation layer: nonequilibrium carriers are generated both at the surface of a crystal and on the inner boundary of the skin layer.

The system of basic equations includes Eqs. (1.5) and (1.11) and the Maxwell equations. The order of this system is, in accordance with Eq. (1.11), a function of the number of groups. We shall find later that the important case is that of strong magnetic fields when $\omega_c\tau_p \gg 1$. It is well known (see[65], §27) that, in this limit, the asymptotic behavior of the transport coefficients is different for "even" and "odd" metals (those with $n = p$ and $n \neq p$). Therefore, a simple model of isotropic electron and hole bands, which we shall use (following[67]) to illustrate the main results, is quite adequate in the case of semimetals.

We shall assume that static and alternating magnetic fields H and $\tilde{\mathrm{H}}$ are both parallel to $z$ and the wave vector is oriented along the normal ($\parallel y$). Then, in the classical range corresponding to $\omega_c \ll T$, the dispersion equation for electromagnetic–density waves is of the form[14)]

$$k^4 + \left(\frac{1}{L^2} - \frac{i}{\delta_0^2}\right)k^2 - \frac{i}{\delta^2 L^2} = 0, \qquad (5.1)$$

where $L^2 \equiv L^2(H) = D(H)\tau(\omega)$, $\tau(\omega) = \tau/(1 - i\omega\tau)$; $L$ is the diffusion length; $D(H)$ is the ambipolar diffusion coefficient; $\tau$ is the recombination time; $\omega$ is the frequency of the wave. The skin depths $\delta$ and $\delta_0$ are

$$\frac{1}{\delta_0^2} = \frac{4\pi\omega}{c^2}(\sigma_n^* + \sigma_p^*), \quad \frac{1}{\delta^2} = \frac{4\pi\omega}{c^2}\sigma^*, \qquad (5.2)$$

where $\sigma^*$ and $\sigma_{n,p}^*$ are given by Eqs. (1.2) and (1.9). If $a \sim \omega_c\tau_p \gg 1$, the conductivities are $\sigma^* \sim \sigma/a^2$ and $\sigma_{n,p}^* \sim \sigma^*$, and $\delta \sim a\delta_0 \gg \delta_0$; we then also have $D(H) \sim D(0)/a^2$ and $L \sim L(0)/a$. The quantity $\delta$ is the classical skin depth of an even metal and $\delta_0$ is the corresponding depth of an odd metal. Equation (5.1) applies to the normal skin depth, i.e., for $kr_L \ll 1$ (this is the local limit[123] of the validity of the phenomenological theory).

Since $\delta/\delta_0 \sim a \gg 1$, the roots of Eq. (5.1) are quite different: $|k_1|^2 \gg |k_2|^2$. Their values depend on the parameter

$$\left(\frac{L}{\delta_0}\right)^2 = \frac{8\pi n}{3H^2}(\varepsilon_{Fn} + \varepsilon_{Fp})\,\omega\tau(\omega). \qquad (5.3)$$

We shall now consider two limiting cases.

Case A corresponds to

$$\left(\frac{L}{\delta_0}\right)^2 \ll 1, \quad k_1^2 = -\frac{1}{L^2}, \quad k_2^2 = \frac{i}{\delta^2}. \qquad (5.4a)$$

Case B corresponds to

$$\left(\frac{L}{\delta_0}\right)^2 \gg 1, \quad k_1^2 = \frac{i}{\delta_0^2}, \quad k_2^2 = -\left(\frac{\delta_0}{\delta L}\right)^2 \sim \frac{1}{D(0)\tau}. \qquad (5.4b)$$

We can see immediately that the depths of penetration of the waves are equal to the diffusion length $L$ and to the skin depth $\delta$ only if $L \ll \delta_0$. On the other hand, if $L \gg \delta_0$, they reduce to the values corresponding to $H = 0$.

---

[14)]In general, the degree of the dispersion equation is $2\nu$.

The ratio of the amplitudes of the two excited waves and, consequently, the surface impedance $Z$ depend on the surface recombination velocity:

case A

$$Z=Z_0\begin{cases}[1-(i^{3/2}L\delta/\delta_0^2)]^{-1}, & s=0,\\ 1, & s=\infty;\end{cases} \tag{5.5a}$$

case B

$$Z=Z_0\frac{\delta_0}{\delta}\begin{cases}1, & s=0,\\ 1+(i^{1/2}\delta/L), & s=\infty;\end{cases} \tag{5.5b}$$

here, $Z_0=4\pi\omega\delta/i^{1/2}c^2$ is the usual expression for the impedance which is obtained in the absence of anisotropic size effects. We can see that Eq. (5.5) gives this impedance only in case A when additional conditions are satisfied: either $s=\infty$ or $L(0)\ll\delta_0$.

Thus, under conditions corresponding to the normal skin effect, there is a wide range of fields and frequencies in which anisotropic size effects alter the depth of penetration of the field and surface impedance by an order of magnitude, depending on the anisotropy parameter $a\gg 1$. Naturally, the size effects occur also in $H=0$: their magnitude is governed by the parameters $a_\alpha$ of the individual valleys.[19] In the anomalous skin effect case, the Sondheimer results[124] are basically retained and the influence of anisotropic size effects is confined to corrections which do not exceed $\delta/L$.[19]

In the quantum range, $\omega_c\gtrsim T$, there is an additional mechanism of nonequilibrium carrier generation, which is the quantum dependence of the carrier density $n(B)$ on the magnetic induction $B$. At the same time, oscillations of the premeability $\mu=dB/dH$ become important in electrodynamics.[125,126] A phenomenological theory of the quantum range is developed in[127]. We shall not analyze the waves but note only that the formula for $(L/\delta_0)^2$, similar to Eq. (5.3), now includes $\mu(B)$ and the full range of the parameters corresponding to cases A and B above can be covered in one quantum oscillation if its amplitude is sufficiently large.

## B. Electromagnetic excitation of sound[15)]

The deformation potential of conduction electrons depends on the electron momentum $\hat{\Lambda}=\hat{\Lambda}(\mathbf{p})$. Therefore, a change in the electron distribution function alters the lattice energy and the gradient of the distribution function produces a bulk force acting on the lattice. This mechanism of the interaction of electrons with the lattice is known as the deformation interaction.[128–130] In semimetals, each valley has its own deformation potential $\hat{\Lambda}_\alpha$, which can be assumed to be independent of the momentum.

The deformation interaction causes an electromagnetic-density wave to generate an inhomogeneous force which acts on the lattice and which should excite acoustic waves. The conversion coefficient $\Gamma$, defined as the ratio of the energy fluxes in the acoustic and electromagnetic waves, can be described most simply[16)] for long acoustic waves $k_s=\omega/c_s\ll k_1$, $k_2$[131–133]:

$$\Gamma=\frac{9H^2}{16\pi\rho c c_s}\left(a_n a_p k_s^2 L^2\frac{\Lambda_n-\Lambda_p}{\varepsilon_{F_n}+\varepsilon_{F_p}}\right)^2|g|^2 \tag{5.6}$$

where $\rho$ is the density and

$$g=\begin{cases}[1+(\delta L/\sqrt{i}\,\delta_0^2)]^{-1}, & s=0, \quad (5.7a)\\ 1, & s=\infty. \quad (5.7b)\end{cases}$$

In both case A and B [compare with Eq. (5.4)], we have $\Gamma\propto H^2$ but with different coefficients. The temperature dependence of $\Gamma$ is governed by the temperature dependences of $\tau(\omega)$ and of the mean free time $\tau_p$. If $s=\infty$, and also if $s=0$ and $L\delta/\delta_0^2\ll 1$, we have $\Gamma\propto\tau_p^2\tau^2(\omega)$. If $s=0$, we find that if $L\delta/\delta_0^2\gg 1$ (case A) and, in case B, we obtain $\Gamma\propto\tau(\omega)$.

In addition to the deformation mechanism, there is always the ponderomotive mechanism of the excitation of sound([135], §34). If $k_s\ll k_1$, $k_2$, which is the case we shall discuss here, the ponderomotive mechanism gives $\Gamma\propto H^2$ and the conversion coefficient is independent of temperature. In semimetals, the relative importance of this mechanism is small because of the large factor $\Lambda_n-\Lambda_p)^2/\ _F^2\sim 10^4$ (see[136]) which occurs in Eq. (5.6).

Experimental investigations of the electromagnetic excitation of sound in semimetals were started in[137] with Bi in which the effect was observed beginning from fields $H\sim 10$ Oe. The sample acted as an acoustic resonator and the effect was deduced from the characteristics of the surface impedance corresponding to the excitation of standing waves. It was later suggested[138] that the high-intensity sound was not excited because of the ponderomotive mechanism but was due to the intervalley redistribution of the type described in[16,57]. The generation of sound was investigated later in[132,138–140] and interpreted in[131].

Figure 29 shows the dependence of the intensity of sound $I$ on $H$ and Fig. 30 gives the temperature dependence of $I$. We shall follow here mainly the analysis of these results given in[132].

The absolute value of this effect in Sb was described by $\tau\approx 10^{-8}$ sec. For the values of $H$ in Figs. 29b and 30b, this gave—subject to Eq. (5.3)—an estimate $(L/\delta_0)^2\sim 10$ corresponding to B. The field dependence of $I$ (Fig. 29b) was close to the theoretical relationship $I\propto H^2$. The absence of a temperature dependence in the range $T\lesssim 4$ °K under conditions such that $\tau_p$ depended strongly on temperature clearly indicated that $s$ was small ($s\approx 0$), so that $I\propto\Gamma\propto\tau(\omega)$. The behavior of $I$ at higher temperatures corresponded to a fall of $\tau$ by a factor of about 5 at 10 °K.

It is known that $\tau\sim 10^{-8}$ sec for Bi.[5,71] In the case

15)The propagation of sound in many-valley systems (including absorption, amplification, acoustoelectric and acoustomagnetoelectric effects) itself has a number of interesting features and includes processes which, in some respect, are similar to those discussed in the present review. However, there is no space to consider this important subject. We shall discuss the excitation of sound simply as a method of detecting anisotropic size effects in the presence of a skin layer.

16)In thin samples, the conversion of acoustic waves back into electromagnetic waves may become important and, therefore, it may be necessary to provide a self-consistent analysis.[134]

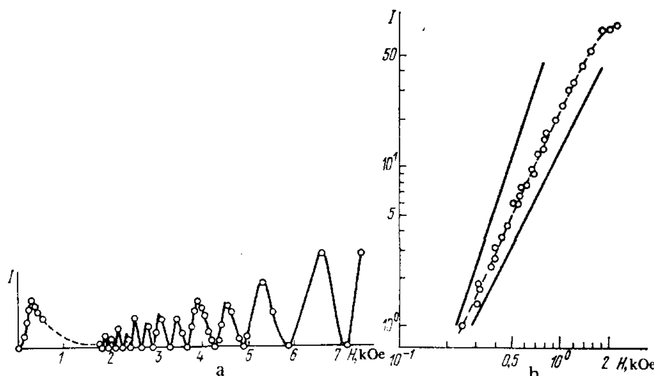

FIG. 29. Dependences of the amplitude of the acoustic resonance on the magnetic field at $T=4.2\,°K$ a) Bi, $\omega/2\pi=0.51$ MHz[138]; b) Sb, $\omega/2\pi=2.8$ MHz[132]; the continuous lines correspond to $I\propto H^2$ and $I\propto H^3$.

of the parameters in Figs. 29a and 30a, this gives $(L/\delta_0)^2\sim 0.1$ (case A) and $L\delta/\delta_0^2\sim 1$. The dependence $I(T)$ in the range 2–4 °K (Fig. 30a) is in qualitative agreement with the dependence $I\propto \tau_p^2\tau^2$, which predicts a fall of $I$ by a factor of 6. The assumption that $s$ is large helps to explain this dependence.[17)] An interesting dependence $I(H)$ is plotted in Fig. 29a. The maximum of $I$ at $H\approx 300$ Oe corresponds to $k_s\sim k_2$; a further increase in the depth of the skin layer reduces $I$ in accordance with the theory.[132,133]

Oscillations in the range $H\lesssim 2$ kOe are a quantum phenomenon, which is analyzed theoretically in[138,141].

The good qualitative agreement between the theory and experiment leaves no doubt about the validity of the adopted interpretation. Therefore, there is every reason to consider the experiments reported in[137] and later as the detection of anisotropic size effects by the excitation of acoustic waves. A direct experimental investigation of the behavior of the impedance, which would make it possible to check formulas such as (5.5), has not yet been carried out (to our knowledge). The dependence of the impedance $Z$ on the frequency and magnetic field should differ considerably from the standard dependence in the case of the normal skin effect. Therefore, it would be interesting to measure the impedance under controlled surface conditions.

## CONCLUSIONS

We shall conclude by summarizing the results obtained and try to define the range of phenomena which we regard as anisotropic size effects. This is not so simple because they are closely linked to a number of related phenomena.

The anisotropy of electronic properties results in transverse electron currents and, consequently, produces circulation (eddy) currents. They are well known in the theory of the thermoelectric power,[142,143] Kikoin–Noskov photomagnetic emf,[144] transverse Dember photo-emf,[145,146] etc. We shall include in the category of anisotropic effects also the phenomena (discussed above) in which the transverse currents create nonequilibrium carrier densities in macroscopic regions. More exactly, these are the phenomena in which the appearance of density gradients has been demonstrated experimentally or theoretically.

The theory developed for specific phenomena has a number of limitations. All the dimensions are assumed to be macroscopically large, so that there are no quantum size effects.[147,148] Electric fields (both weak and "strong") are assumed to be nonheating; this is an important limitation in those cases when anisotropic size effects disappear with rising temperature.

On the other hand, the theory has a fairly wide range of validity and covers anisotropic size effects associated with several "large" relaxation lengths, which are the recombination, intervalley, and cooling lengths, and it can easily be extended to other cases. Certain consequences follow from the theory and these can be compared directly with experiment: the size dependence of the electrical conductivity (including its dependence on the orientation even in cubic crystals and the specific dependence on the state of the surface), appearance of a transverse electric field, nonlinearity of the electrical conductivity in a relatively weak field, giant redistribution of carriers in "strong" fields (accompanied by the formation of accumulation and depletion layers, domains, etc), changes ( by an order of magnitude) in the surface impedance of semimetals, strong electromagnetic excitation of sound, and so on.

Some experiments were carried out before the development of the theory but the majority after and some of the consequences have not yet been subjected to an experimental test. On the whole, the agreement between theory and experiment is satisfactory. However, the interpretation of some of the experiments on the basis of the theory of anisotropic size effects is only qualitative or even tentative; difficulties are encountered in the explanations of some of the experiments. The main features of the above analysis can be stated as follows.

In semiconductors, the recombination length $L_r$ reaches values $L_r\sim 1$ mm. Therefore, extensive experimental studies of anisotropic size effects over distances $L_r$ are absolutely reliable and their comparison with the theory gives fully convincing results (Sec. 3). Here, there are

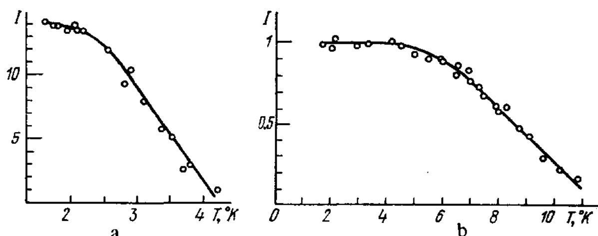

FIG. 30. Temperature dependences of the amplitude of the acoustic resonance: a) Bi, $\omega/2\pi=0.51$ MHz, $H=140$ Oe[138]; b) Sb, $\omega/2\pi=2.8$ MHz, $H=1200$ Oe.[132]

[17)]The conclusion $s_{Bi}\gg s_{Sb}$ was reached independently in[81,83] from an analysis of the size effect.

no unsolved physical problems and such effects have now entered the stage of technical applications.

The situation is much more complex in the case of anisotropic size effects over distances equal to the intervalley length $L_v$ or the cooling length $L_\varepsilon$. At temperatures $T \approx 20-77$ °K, it is estimated that $L_v$ and $L_r$ are of the order of 1–30 $\mu$. Studies of plates containing accumulation layers of this thickness are difficult for a number of reasons; therefore, the precision of the results is not yet high. A quantitative analysis of the experiments is difficult because, in some cases, we have $L_v \approx L$ and anisotropic size effects over both the distances overlap. However, the general conclusion to be drawn from the experimental results is this: anisotropic size effects have been found in the electrical conductivity and magnetoresistance (Secs. 2A and 2E). Unfortunately, no observations have yet been reported of a very interesting pattern of anisotropic size effects which should occur over distances $L_v$ in "strong" fields (Sec. 4); experiments of this kind can be carried out successfully only at low temperatures and in sufficiently pure samples.

In the case of semimetals such as Bi, we have $L_v \approx L_r$; in pure Bi at $T \approx 4$ °K, $L_v$ reaches ~1 mm. In spite of the large value of $L_v$, there is a considerable scatter of the results in studies of the size effect of the electrical conductivity and this is evidently due to purely experimental difficulties in preparing sufficiently perfect oriented samples and establishing standard conditions on their surfaces. Therefore, experimental studies should be made of the transverse electric field and electromagnetic excitation of sound: their interpretation in terms of anisotropic size effects is practically identical (Sec. 5).

*Note added in proof.* Investigations of the anisotropic redistribution of carriers accompanied by the violation of the quasineutrality condition were recently reported.[160,161] The considerable nonlinear change in the conductivity in this case appears either because of changes in the populations of deep centers,[160] which may be present in the bulk or on the surface, or due to a change in the carrier mobility across a sample.[161] The latter effect was observed experimentally.


[1]K. Fuchs, Proc. Cambridge Philos. Soc. 34, 100 (1937).
[2]G. Weinreich, T. M. Sanders Jr, and H. G. White, Phys. Rev. 114, 33 (1959).
[3]W. P. Mason and T. B. Bateman, Phys. Rev. 134, A1387 (1964).
[4]B. Tell and G. Weinreich, Phys. Rev. 143, 584 (1966).
[5]A. A. Lopez, Phys. Rev. 175, 823 (1968).
[6]G. L. Bir and G. E. Pikus, Simmetriya i deformatsionye effekty v poluprovodnikakh (Symmetry and Deformation Effects in Semiconductors), Nauka, M., 1972, p. 485.
[7]R. H. Fowler, Statistical Mechanics, 2nd ed., Cambridge University Press (1936).
[8]H. Welker, Z. Naturforsch. Teil A6, 184 (1951).
[9]E. Weisshaar and H. Welker, Z. Naturforsch. Teil A8, 681 (1953).
[10]O. Madelung, L. Tewordt, and H. Welker, Z. Naturforsch. Teil A 10, 476 (1955).
[11]E. Weisshaar, Z. Naturforsch. Teil A10 488 (1955).
[12]G. E. Pikus, Zh. Tekh. Fiz. 26, 22, 36 (1956) [Sov. Phys. Tech. Phys. 1, 17, 32 (1956)].
[13]F. G. Bass and I. M. Tsidil'kovskiĭ, Zh. Eksp. Teor. Fiz. 28, 312 (1955) [Sov. Phys. JETP 1, 267 (1955)].
[14]É. I. Rashba, Fiz. Tverd. Tela (Leningrad) 6, 3247 (1964) [Sov. Phys. Solid State 6, 2597 (1965)].
[15]I. I. Boĭko, I. P. Zhad'ko, É. I. Rashba, and V. A. Romanov, Fiz. Tverd. Tela (Leningrad) 7, 2239 (1965) [Sov. Phys. Solid State 7, 1806 (1966)].
[16]É. I. Rashba, Zh. Eksp. Teor. Fiz. 48, 1427 (1965) [Sov. Phys. JETP 21, 954 (1965)].
[17]S. H. Köenig, Helv. Phys. Acta 34, 765 (1961).
[18]S. Tosima and T. Hattori, J. Phys. Soc. Jpn. 19, 2022 (1964).
[19]G. I. Babkin and V. Ya. Kravchenko, Zh. Eksp. Teor. Fiz. 57, 1392 (1969) [Sov. Phys. JETP 30, 754 (1970)].
[20]Z. S. Gribnikov and V. I. Mel'nikov, Zh. Eksp. Teor. Fiz. 51, 1909 (1966) [Sov. Phys. JETP 24, 1282 (1967)].
[21]Z. S. Gribnikov, Ukr. Fiz. Zh. 16, 772 (1971).
[22]Yu. I. Gorkun, V. S. Lysenko, V. G. Litovchenko, and V. A. Novominskii, Phys. Status Solidi A3, K281 (1970); Yu. I. Gorkun, V. G. Litovchenko, V. S. Lysenko, and V. A. Novominskii, Phys. Status Solidi A20, 275 (1973).
[23]Z. S. Gribnikov and N. A. Prima, Fiz. Tekh. Poluprovodn. 5, 1274 (1971) [Sov. Phys. Semicond. 5, 1126 (1972)].
[24]V. S. Bochkov and Yu. G. Gurevich, Fiz. Tverd. Tela (Leningrad) 11, 714 (1969) [Sov. Phys. Solid State 11, 570 (1969)].
[25]M. Ya. Azbel', Zh. Eksp. Teor. Fiz. 44, 1262 (1963) [Sov. Phys. JETP 17, 851 (1963)].
[26]N. A. Prima, Fiz. Tekh. Poluprovodn. 9, 2036 (1975) [Sov. Phys. Semicond. 9, 1332 (1975)].
[27]N. A. Prima, Fiz. Tekh. Poluprovodn. 7, 338 (1973) [Sov. Phys. Semicond. 7, 241 (1973)].
[28]F. G. Bass, V. S. Bochkov, and Yu. G. Gurevich, Fiz. Tverd. Tela (Leningrad) 9, 3479 (1967) [Sov. Phys. Solid State 9, 2742 (1968)].
[29]M. I. Belinskiĭ and Z. S. Gribnikov, Ukr. Fiz. Zh. 14, 1233 (1969).
[30]A. I. Klimovskaya, Fiz. Tekh. Poluprovodn. 7, 637 (1973) [Sov. Phys. Semicond. 7, 444 (1973)].
[31]E. M. Conwell, High Field Transport in Semiconductors, Suppl. 9 to Solid State Phys., Academic Press, New York (1967).
[32]V. A. Kochelap and V. V. Mitin, Fiz. Tekh. Poluprovodn. 4, 1051 (1970) [Sov. Phys. Semicond. 4, 896 (1970)].
[33]N. A. Prima, Ukr. Fiz. Zh. 21, 317 (1976).
[34]V. V. Mitin and N. A. Prima, Phys. Status Solidi B58, 809 (1973).
[35]Z. S. Gribnikov and É. I. Rashba, Fiz. Tverd. Tela (Leningrad) 9, 967 (1967) [Sov. Phys. Solid State 9, 760 (1967)].
[36]Z. S. Gribnikov, V. I. Mel'nikov, and T. S. Sorokina, Fiz. Tverd. Tela (Leningrad) 8, 3379 (1966) [Sov. Phys. Solid State 8, 2699 (1967)].
[37]F. G. Bass, V. S. Bochkov, and Yu. G. Gurevich, Fiz. Tekh. Poluprovodn. 7, 3 (1973) [Sov. Phys. Semicond. 7, 1 (1973)].
[38]A. I. Klimovskaya and O. V. Snitko, Pis'ma Zh. Eksp. Teor. Fiz. 7, 194 (1968) [JETP Lett. 7, 149 (1968)].
[39]A. I. Klimovskaya, O. V. Snitko, and V. I. Mel'nikov, Proc. Ninth Intern. Conf. on Physics of Semiconductors, Moscow, 1968, Vol. 2, publ. by Nauka, Leningrad (1968), p. 801.
[40]A. I. Klimovskaya, S. I. Kirillova, and O. V. Snitko, Fiz. Tekh. Poluprovodn. 8, 448 (1974)].
[41]B. P. Zot'ev, A. F. Kravchenko, and É. M. Skok, Fiz. Tekh. Poluprovodn. 6, 1377 (1972) [Sov. Phys. Semicond. 6, 1200 (1972)].
[42]V. E. Primachenko, O. V. Snitko, and V. V. Milenin, Phys. Status Solidi 11, 711 (1965).
[43]W. A. Albers Jr and J. E. Thomas Jr, J. Phys. Chem. Solids 14, 181 (1960).

[44]M. H. Brodsky and R. B. Schoolar, J. Appl. Phys. 40, 107 (1969).
[45]P. P. Vil'ms, V. S. Sardaryan, P. P. Dobrovol'skiĭ, and S. V. Kapylova, Pis'ma Zh. Eksp. Teor. Fiz. 10, 377 (1969) [JETP Lett. 10, 240 (1969)].
[46]V. S. Sardaryan, P. P. Vil'ms, É. A. Klimenko, A. G. Klimenko, and K. T. Ermaganbetov, Fiz. Tekh. Poluprovodn. 3, 1255 (1969) [Sov. Phys. Semicond. 3, 1051 (1970)].
[47]V. S. Sardaryan and P. P. Vil'ms, Fiz. Tekh. Poluprovodn. 4, 1375 (1970) [Sov. Phys. Semicond. 4, 1168 (1971)].
[48]B. P. Zot'ev, A. F. Kravchenko, É. M. Skok, and K. T. Ermaganbetov, Fiz. Tekh. Poluprovodn. 6, 1077 (1972) [Sov. Phys. Semicond. 6, 937 (1972)].
[49]T. N. Sitenko, V. I. Lyashenko, and I. P. Tyagulskii, Phys. Status Solidi A 9, 51 (1972).
[50]B. P. Zot'ev, A. F. Kravchenko, É. M. Skok, and V. I. Yudaev, Fiz. Tekh. Poluprovodn. 6, 1072 (1972) [Sov. Phys. Semicond. 6, 933 (1972)].
[51]C. Herring, J. Appl. Phys. 31, 1939 (1960).
[52]A. I. Klimovskaya, O. V. Snitko, and S. I. Kirillova, Pis'ma Zh. Eksp. Teor. Fiz. 11, 119 (1970) [JETP Lett. 11, 73 (1970)]; Fiz. Tekh. Poluprovodn. 5, 1281 (1971) [Sov. Phys. Semicond. 5, 1131 (1972)].
[53]A. I. Klimovskaya, S. I. Kirillova, and O. V. Snitko, Fiz. Tekh. Poluprovodn. 8, 707 (1974) [Sov. Phys. Semicond. 8, 451 (1974)].
[54]W. S. Boyle and G. E. Smith, Prog. Semicond. 7, 1 (1963).
[55]L. A. Fal'kovskiĭ, Usp. Fiz. Nauk 94, 3 (1968) [Sov. Phys. Usp. 11, 1 (1968)].
[56]Yu. I. Gorkun and É. I. Rashba, Fiz. Tverd. Tela (Leningrad) 10, 3053 (1968) [Sov. Phys. Solid State 10, 2406 (1969)].
[57]V. Ya. Kravchenko and É. I. Rashba, Zh. Eksp. Teor. Fiz. 56, 1713 (1969) [Sov. Phys. JETP 29, 918 (1969)].
[58]M. Ya. Azbel' and V. G. Peschanskiĭ, Zh. Eksp. Teor. Fiz. 49, 572 (1965) [Sov. Phys. JETP 22, 399 (1966)]; V. G. Peschanskiĭ and M. Ya. Azbel', Zh. Eksp. Teor. Fiz. 55, 1980 (1968) [Sov. Phys. JETP 28, 1045 (1969)].
[59]J. E. Parrott, Proc. Phys. Soc. London 85, 1143 (1965).
[60]Yu. I. Gorkun, Ukr. Fiz. Zh. 16, 657 (1971).
[61]R. Engleman and E. H. Sondheimer, Proc. Phys. Soc. London Sec. B69, 449 (1956).
[62]F. S. Ham and D. C. Mattis, IBM J. Res. Dev. 4, 143 (1960).
[63]P. J. Price, IBM J. Res. Dev. 4, 152 (1960).
[64]J. E. Parrott, Proc. Phys. Soc. London 87, 1000 (1966).
[65]I. M. Lifshits, M. Ya. Azbel', and M. I. Kaganov, Élektronnaya teoriya metallov, Nauka, M., 1971 (Electron Theory of Metals, Consultants Bureau, New York, 1973).
[66]T. Hattori, J. Phys. Soc. Jpn. 23, 19 (1967).
[67]G. I. Babkin and V. Ya. Kravchenko, Zh. Eksp. Teor. Fiz. 60, 695 (1971) [Sov. Phys. JETP 33, 378 (1971)].
[68]A. N. Friedman and S. H. Köenig, IBM J. Res. Dev. 4, 158 (1960).
[69]R. Hartman, Phys. Rev. 181, 1070 (1969).
[70]R. N. Zitter, Phys. Rev. Lett. 14, 14 (1965).
[71]A. N. Friedman, Phys. Rev. 159, 553 (1967).
[72]N. Garcia and Y. H. Kao, Phys. Lett. A 26, 373 (1968).
[73]G. E. Smith, Phys. Rev. 115, 1561 (1959).
[74]M. S. Khaĭkin and V. S. Édel'man, Zh. Eksp. Teor. Fiz. 47, 878 (1964) [Sov. Phys. JETP 20, 587 (1965)].
[75]J. E. Aubrey and C. J. Creasey, J. Phys. C 2, 824 (1969).
[76]J. E. Parott, J. Phys. F 1, 657 (1971).
[77]É. S. Medvedev, V. N. Kopylov, and L. P. Mezhov-Deglin, Fiz. Nizkikh Temp. 1, 1192 (1975) [Sov. J. Low Temp. Phys. 1, 572].
[78]J. E. Aubrey and A. J. Barreu, J. Phys. F 1, L36 (1971).
[79]I. N. Zhilyaev and L. P. Mezhov-Deglin, Pis'ma Zh. Eksp. Teor. Fiz. 19, 461 (1974) [JETP Lett. 19, 248 (1974)].
[80]I. N. Zhilyaev and L. P. Mezhov-Deglin, Zh. Eksp. Teor. Fiz. 70, 971 (1976) [Sov. Phys. JETP 43, (1976)].
[81]Yu. A. Bogod and V. B. Krasovitskiĭ, Phys. Status Solidi B 65, 847 (1974).
[82]Yu. A. Bogod, B. I. Verkin, and V. B. Krasovitskiĭ, Zh. Eksp. Teor. Fiz. 61, 275 (1971) [Sov. Phys. JETP 34, 142 (1972)].
[83]Yu. A. Bogod and V. B. Krasovitskiĭ, Zh. Eksp. Teor. Fiz. 63, 1036 (1972) [Sov. Phys. JETP 36, 544 (1973)].
[84]V. E. Lashkarev, Zh. Eksp. Teor. Fiz. 18, 953 (1948).
[85]E. I. Rashba, V. A. Romanov, I. I. Boiko, and I. P. Zhadko, Phys. Status Solidi 16, 44 (1966).
[86]I. P. Zhad'ko, V. A. Romanov, É. I. Rashba, and I. I. Boĭko, Fiz. Tekh. Poluprovodn. 1, 1174 (1967) [Sov. Phys. Semicond. 1, 982 (1968)].
[87]V. A. Romanov, I. P. Zhadko, and I. I. Boiko, Phys. Status Solidi 17, 389 (1966).
[88]I. S. Levitas, Yu. K. Pozhela, and A. P. Sashchuk, Fiz. Tekh. Poluprovodn. 6, 205 (1972) [Sov. Phys.-Semicond. 6, 175 (1972)].
[89]V. K. Malyutenko, G. I. Teslenko, and I. I. Boĭko, Fiz. Tekh. Poluprovodn. 8, 916 (1974) [Sov. Phys. Semicond. 8, 590 (1974)].
[90]I. P. Zhad'ko, Ukr. Fiz. Zh. 12, 1387 (1967).
[91]I. P. Zhad'ko, V. A. Romanov, B. K. Serdega, and Yu. G. Yurov, Ukr. Fiz. Zh. 19, 1682 (1974).
[92]I. P. Zhad'ko, V. A. Romanov, B. K. Serdega, and L. S. Solonchuk, Fiz. Tekh. Poluprovodn. 9, 297 (1975) [Sov. Phys. Semicond. 9, 193 (1975)].
[93]A. I. Ansel'm, Zh. Tekh. Fiz. 22, 1146 (1952).
[94]R. W. Landauer and J. Swanson, Phys. Rev. 91, 555 (1953).
[95]P. B. Banbury, H. K. Henisch, and A. Many, Proc. Phys. Soc. London Sec. A 66, 753 (1953).
[96]A. Chovet and G. Kamarinos, Rev. Phys. Appl. 6, 345 (1971).
[97]M. Bernard, J. Phys. Chem. Solids 8, 332 (1959).
[98]A. C. Beer, Galvanomagnetic Effects in Semiconductors, Suppl. 4 to Solid State Phys., Academic Press, New York, p. 60.
[99]I. I. Boiko. I. P. Zhadko, and V. A. Romanov, Phys. Status Solidi 34, 461 (1969).
[100]A. P. Varyakoite (A. Variakojyte), I. S. Levitas, and Yu. K. Pozhela (J. Pozela), Lit. Fiz. Sb. 6, 429 (1966).
[101]I. S. Levitas, Yu. K. Pozhela, and R. F. Fikhman, Fiz. Tekh. Poluprovodn. 1, 410 (1967) [Sov. Phys. Semicond. 1, 337 (1967)].
[102]V. V. Mitin, Fiz. Tekh. Poluprovodn. 5, 1729 (1971) [Sov. Phys. Semicond. 5, 1511 (1972)].
[103]Z. S. Gribnikov, G. I. Lomova, and V. A. Romanov, Phys. Status Solidi 28, 815 (1968).
[104]Z. S. Gribnikov, I. P. Zhad'ko, V. A. Romanov, and B. K. Serdega, Ukr. Fiz. Zh. 15, 303 (1970); Phys. Status Solidi 35, K163 (1969).
[105]É. I. Rashba and K. B. Tolpygo, Zh. Tekh. Fiz. 26, 1419 (1956) [Sov. Phys. Tech. Phys. 1, 1388 (1957)].
[106]M. A. Lampert and A. Rose, Phys. Rev. 121, 26 (1961); A. Rose, J. Appl. Phys. 35, 2664 (1964).
[107]R. Hirota, S. Tosima, and M. A. Lampert, J. Phys. Soc. Jpn. 18, 535 (1963).
[108]Z. S. Gribnikov, Fiz. Tverd. Tela (Leningrad) 7, 251 (1965) [Sov. Phys. Solid State 7, 191 (1965)].
[109]V. I. Stafeev, Fiz. Tverd. Tela (Leningrad) 1, 841 (1959). [Sov. Phys. Solid State 1, 763 (1959)].
[110]É. I. Karakushan and V. I. Stafeev, Fiz. Tverd. Tela Leningrad) 3, 677 (1961) [Sov. Phys. -Solid State 3, 493 (1961)].
[111]L. E. Vorob'ev, É. I. Karakushan, and V. I. Stafeev, Fiz. Tverd. Tela (Leningrad) 5, 982 (1963) [Sov. Phys. Solid State 5, 715 (1963)].
[112]T. Yamada, Proc. Ninth Intern. Conf. on Physics of Semiconductors, Moscow, 1968, Vol. 2, publ. by Nauka, Leningrad (1968), p. 672.
[113]H. Pfleiderer, Solid-State Electron. 15, 335 (1972); 16, 1347 (1973).

[114]B. Robinson, in: Current Injection in Solids (ed. by M. A. Lampert and P. Mark), Academic Press, New York, 1970 (Russ. Transl., Mir, M., 1973, p. 282).
[115]J. F. Schetzina and J. P. McKelvey, Phys. Rev. B 2, 1869 (1970).
[116]Z. S. Gribnikov, Fiz. Tekh. Poluprovodn. 9, 1740 (1975) [Sov. Phys. Semicond. 9, 1143 (1975)].
[117]Z. S. Gribnikov, V. A. Kochelap, and É. I. Rashba, Zh. Eksp. Teor. Fiz. 51, 266 (1966) [Sov. Phys. JETP 24, 178 (1967)]; Fiz. Tverd. Tela (Leningrad) 8, 2479 (1966) [Sov. Phys. Solid State 8, 1981 (1967)].
[118]É. I. Rashba, I. I. Boiko, V. A. Kochelap (Cochelap), Z. S. Gribnikov, V. A. Romanov, and I. P. Zhad'ko, Proc. Eighth Intern. Conf. on Physics of Semiconductors, Kyoto, 1966, in: J. Phys. Soc. Jpn. 21, Suppl., 351 (1966).
[119]Z. S. Gribnikov and V. V. Mitin, Ukr. Fiz. Zh. 14, 240 (1969).
[120]Z. S. Gribnikov, Pis'ma Zh. Eksp. Teor. Fiz. 9, 545 (1969) [JETP Lett. 9, 332 (1969)].
[121]Z. S. Gribnikov, Fiz. Tekh. Poluprovodn. 3, 1821 (1969) [Sov. Phys. Semicond. 3, 1543 (1970)].
[122]The Physics of Semimetals and Narrow-Gap Semiconductors (Proc. Conf., Dallas, Texas, 1970), in: J. Phys. Chem. Solids 32, Suppl. 1 (1971).
[123]É. A. Kaner and V. G. Skobov, Usp. Fiz. Nauk 89, 367 (1966) [Sov. Phys. Usp. 9, 480 (1967)].
[124]E. H. Sondheimer, Proc. R. Soc. Ser. A 224, 260 (1954).
[125]M. Ya. Azbel' and G. A. Begiashvili, Pis'ma Zh. Eksp. Teor. Fiz. 3, 201 (1966) [JETP Lett. 3, 128 (1966)].
[126]R. G. Mints, Pis'ma Zh. Eksp. Teor. Fiz. 11, 128 (1970) [JETP Lett. 11, 79 (1970)].
[127]V. Ya. Kravshenko and É. I. Rashba, Zh. Eksp. Teor. Fiz. 61, 753 (1971) [Sov. Phys. JETP 34, 403 (1972)].
[128]A. I. Akhiezer, M. I. Kaganov, and G. Ya. Lyubarskiĭ, Zh. Eksp. Teor. Fiz. 32, 837 (1957) [Sov. Phys. JETP 5, 685 (1957)].
[129]V. L. Gurevich, Zh. Eksp. Teor. Fiz. 37, 71, 1680 (1959) [Sov. Phys. JETP 10, 51, 1190 (1960)].
[130]V. M. Kontorovich, Zh. Eksp. Teor. Fiz. 45, 1638 (1963) [Sov. Phys. JETP 18, 1125 (1964)].
[131]G. I. Babkin, V. T. Dolgopolov and V. Ya. Kravchenko, Pis'ma Zh. Eksp. Teor. Fiz. 13, 563 (1971) [JETP Lett. 13, 402 (1971)].
[132]V. T. Dolgopolov, Zh. Eksp. Teor. Fiz. 61, 1545 (1971) [Sov. Phys. JETP 34, 823 (1972)].
[133]G. I. Babkin and V. Ya. Kravchenko, Zh. Eksp. Teor. Fiz. 61, 2083 (1971) [Sov. Phys. JETP 34, 1111 (1972)].
[134]I. A. Gilinskiĭ, M. B. Sultanov, and Yu. V. Levin, Zh. Eksp. Teor. Fiz. 66, 225 (1974) [Sov. Phys. JETP 39, 106 (1974)].
[135]L. D. Landau and E. M. Lifshitz, Élektrodinamika sploshnykh sred, Gostekhizdat, M., 1957 (Electrodynamics of Continuous Media, Pergamon Press, Oxford, 1960).
[136]K. Walther, Phys. Rev. 174, 782 (1968).
[137]V. F. Gantmakher and V. T. Dogopolov, Pis'ma Zh. Eksp. Teor. Fiz. 5, 17 (1967) [JETP Lett. 5, 12 (1967)].
[138]V. F. Gantmakher and V. T. Dolgopolov, Zh. Eksp. Teor. Fiz. 57, 132 (1969) [Sov. Phys. JETP 30, 78 (1970)].
[139]E. R. Dobbs, R. L. Thomas, and D. Hsu, Phys. Lett. A 30, 338 (1969).
[140]E. R. Dobbs, J. Phys. Chem. Solids 31, 1657 (1970).
[141]V. Ya. Kravchenko, Zh. Eksp. Teor. Fiz. 62, 377 (1972) [Sov. Phys. JETP 35, 202 (1972)].
[142]V. L. Ginzburg, Zh. Eksp. Teor. Fiz. 14, 177 (1944).
[143]A. G. Samoĭlovich and L. L. Korenblit, Fiz. Tverd. Tela (Leningrad) 3, 2054 (1961) [Sov. Phys. Solid State 3, 1494 (1962)].
[144]B. Ya. Moĭzhes, Zh. Tekh. Fiz. 27, 495 (1957) [Sov. Phys. Tech. Phys. 2, 444 (1958)].
[145]W. van Roosbroeck and W. G. Pfann, J. Appl. Phys. 33, 2304 (1962).
[146]I. P. Zhad'ko, É. I. Rashba, V. A. Ramonov, I. M. Stakhira, and K. D. Tovstyuk, Fiz. Tverd. Tela (Leningrad) 7, 1777 (1965) [Sov. Phys. Solid State 7, 1432 (1965)].
[147]B. A. Tavger and V. Ya. Demikhovskiĭ, Usp. Fiz. Nauk 96, 61 (1968) [Sov. Phys. Usp. 11, 644 (1969)].
[148]V. N. Lutskii, Phys. Status Solidi A 1, 199 (1970).
[149]R. E. Peierls, Quantum Theory of Solids, Clarendon Press, Oxford, 1955 (Russ. Transl., IL, M., 1956), Chap. 6.
[150]R. N. Gurzhi, Usp. Fiz. Nauk 94, 689 (1968) [Sov. Phys. Usp. 11, 255 (1968).
[151]G. E. Pinkus, Osnovy teorii poluprovodnikovykh priborov (Fundamentals of the Theory of Semiconductor Devices), Nauka, M., 1965.
[152]J. S. Blakemore, Semiconductor Statistics, Pergamon Press, Oxford, 1962 (Russ. Transl., Mir, M., 1964), Chap. 10.
[153]R. H. Bube, Photoconductivity of Solids, Wiley, New York, 1960 (Russ. Transl., IL, M., 1962), Sec. 12.
[154]S. M. Ryvkin, Fotoélektricheskie yavleniya v poluprovodnikakh, Fizmatgiz, M., 1963 (Photoelectric Effects in Semiconductors, Consultants Bureau, New York, 1964).
[155]V. N. Kopylov and L. P. Mezhov-Deglin, Zh. Eksp. Teor. Fiz. 65, 720 (1973) [Sov. Phys. JETP 38, 357 (1974)].
[156]V. S. Tsoĭ, a) Zh. Eksp. Teor. Fiz. 68, 1849 (1975) [Sov. Phys. JETP 41, 927 (1975)]; b) Pis'ma Zh. Eksp. Teor. Fiz. 22, 409 (1975) [JETP Lett. 22, 197 (1975)].
[157]V. N. Kopylov and L. P. Mezhov-Deglin, Fiz. Tverd. Tela (Leningrad) 15, 13 (1973) [Sov. Phys. Solid State 15, 8 (1973)].
[158]C. Jacoboni, C. Canali, G. Ottaviani, and A. Alberigi-Quaranta, Proc. Twelfth Intern. Conf. on Physics of Semiconductors, Stuttgart, 1974, publ. by Teubner, Sttuttgart (1974), p. 824.
[159]V. S. Tsoi and I. I. Razgonov, Pis'ma Zh. Eksp. Teor. Fiz. 23, 107 (1976) [JETP Lett. 23, 92 (1976)].
[160]Z. S. Gribnikov and A. V. Sachenko, Fiz. Tekh. Poluprovodn. 10, 304 (1976) [Sov. Phys. Semicond. 10, 182 (1976)].
[161]A. M. Belyantsev, V. A. Valov, and V. A. Kozlov, Zh. Eksp. Teor. Fiz. 70, 569 (1976) [Sov. Phys. JETP 43, (1976)].

Translated by A. Tybulewicz